
# Supplementary Materials for

## VHL Substrate Transcription Factor ZHX2 As An Oncogenic Driver In Clear Cell Renal Cell Carcinoma

Jing Zhang, Tao Wu, Jeremy Simon, Mamoru Takada, Ryoichi Saito, Cheng Fan, Xian-De Liu, Eric Jonasch, Ling Xie, Xian Chen, Xiaosai Yao, Bin Tean Teh, Patrick Tan, Xingnan Zheng, Mingjie Li, Cortney Lawrence, Jie Fan, Jiang Geng, Xijuan Liu, Lianxin Hu, Jun Wang, Chengheng Liao, Kai Hong, Giada Zurlo, Joel S. Parker, J. Todd Auman, Charles M. Perou, W. Kimryn Rathmell, William Y. Kim, Marc W. Kirschner, William G. Kaelin Jr, Albert S. Baldwin, and Qing Zhang

Correspondence to: Qing_Zhang@med.unc.edu

**This PDF file includes:**

## Materials and Methods

Cell Culture and Reagents

786-O, UMRC2, RCC4, UMRC6, and 293T cells were cultured in DMEM containing 10% fetal bovine serum plus 1% penicillin–streptomycin. Following lentivirus infection, cells were maintained in the presence of hygromycin (200 μg/mL) or puromycin (2 μg/mL) depending on the vector. All cells were maintained in an incubator at 37°C and 5% CO2. DMOG (D1070-1g) was from Frontier Scientific, MG132 (IZL-3175-v) was from Peptide International, and DFO (D9533-1G) was from Sigma.

Western Blot Analysis and Antibodies

EBC buffer (50 mM Tris pH 8.0, 120 mM NaCl, 0.5% NP40, 0.1 mM EDTA, and 10% glycerol) supplemented with complete protease inhibitor (Roche Applied Biosciences) was used to harvest whole cell lysates. Subcellular protein fractionation kits were obtained from Thermo Scientific. Cell lysate concentrations were measured by Bradford assay, and equal amounts of cell lysates were resolved by SDS-PAGE. Rabbit ZHX2 antibody (112232) was from Genetex. Mouse anti-HIF2α (ab157249) and rabbit anti-histone 3 (ab1791) antibodies were from Abcam. Mouse ubiquitin antibody was from Santa Cruz Biotechnology (sc-8017). Antibodies against vinculin (V9131) and α-tubulin (T9026) were from Sigma. Rabbit p65 (8242), rabbit RelB (4922), p100/p52 (4882), rabbit cleaved PARP (5625P), rabbit cleaved caspase-3 (9661s), and rabbit FLAG-tag (14793S) antibodies were from Cell Signaling Technology. Mouse antibody against hemagglutinin (MMS-101P) was obtained from Covance. Peroxidase-conjugated goat anti-mouse (31430) and peroxidase-conjugated goat anti-rabbit (31460) secondary antibodies were purchased from Thermo Scientific.

Plasmids

GST-VBC, pBABE HA-VHL, and pcDNA-3.1-FLAG-VHL were previously described (*31, 32*). pcDNA-3.1-HA-ZHX2(WT), pcDNA-3.1-HA-ZHX2(P427A), pcDNA-3.1-HA-ZHX2(P440A), pcDNA-3.1-HA-ZHX2(P464A), pcDNA-3.1-HA-ZHX2 (P427/440/464A), pcDNA-3.1-HA-ZHX2(ZHX2sh45/sg1-resistant), and plenti-UBCp-gateway-FLUC-3×HA-ZHX2 were constructed using standard molecular biology techniques. Quick Change XL Site-Directed Mutagenesis Kit (200516, Agilent Technologies) was used to construct ZHX2 mutants. p65-Flag and p50-Flag were described previously (*33*). All plasmids were sequenced to confirm validity.

siRNAs, Lentiviral shRNA, and sgRNA Vectors

Non-targeting siRNA 2 was obtained from Dharmacon (D0012100220). Lentiviral p65 shRNAs were described previously (*34*). Lentiviral ZHX2 shRNAs were obtained from Broad Institute TRC shRNA library. Target sequences were as follows:
Control shRNA: AACAGTCGCGTTTGCGACTGG
ZHX2 shRNA (43): CCCACTAAATACTACCAAATA
ZHX2 shRNA (44): CGGACATCACAAGTAGTAGAA
ZHX2 sh/siRNA (45): CCGTAGCAAGGAAAGCAACAA
ZHX1 siRNA: CTGACTTTTGATGGTAGTTTT
RelA/p65 shRNA (1): GCCTTAATAGTAGGGTAAGTT
RelA/p65 shRNA (2): CGGATTGAGGAGAAACGTAAA

Control sgRNA: GCGAGGTATTCGGCTCCGCG
ZHX2 sgRNA (1): CATGATACGTGCGACCGTGT
ZHX2 sgRNA(2): GATCACCCCCGAGAACCACG
VHL sgRNA (1): CATACGGGCAGCACGACGCG
VHL sgRNA (2): GCGATTGCAGAAGATGACCT
VHL sgRNA (8): ACCGAGCGCAGCACGGGCCG

Transfection

For immunoblots of cell lysates, qRT-PCR, or soft agar assay, ccRCC cell lines (UMRC2, UMRC6, and RCC4) were seeded on 6-well plates at $3\times10^5$ cells/well (approximately 90-95% confluency). For immunoprecipitation, ccRCC cells were seeded on p100 dishes at $2\times10^6$ cells/dish. Cells were transfected the following day with Lipofectamine 2000 transfection reagent (11668019, Thermo Fisher Scientific). Cells were harvested 48 hours after transfection. siRNAs were transfected with Lipofectamine RNAiMAX transfection reagent. (13778150, Thermo Fisher Scientific).

Virus Production and Infection

293T packaging cell lines were used for lentiviral amplification. Lentiviral infection was carried out as previously described (*35*). Briefly, viruses were collected at 48 h and 72 h post-transfection. After passing through 0.45-μm filters, viruses were used to infect target cells in the presence of 8 μg/mL polybrene. Subsequently, target cell lines underwent appropriate antibiotic selection.

Cell Invasion Assay

BD BioCoat Matrigel Invasion Chambers (354480) were used for 786-O cell invasion assays according to manufacturer's instructions. 786-O cell suspensions were seeded at $4\times10^4$ cells in each chamber in triplicate and incubated for 18 h in an incubator at 37°C in 5% $CO_2$. Cells on the lower surface of the membrane were stained with Diff-Quick stain kit (B4132-1A, Siemens) and counted under an EVOS XL Core microscope (AMEX1000, Thermo Fisher Scientific).

ATP production Assay

ATP production assay was performed by using ATP Bioluminescence Assay Kit HS II (Roche, Cat# 11699709001) following its individual manufacturer's instruction. Cells were harvested 72 hours after seeded on p100 dishes. Then, cells were lysed and diluted to 0.1 μg/μl of protein concentration for measurement of luminescence.

Glucose reserve assay

Cell media was collected 72 hours after seeded on p100 dishes. Glucose reserve assay was performed by using Glucose Assay Kit (Abcam, Cat# ab65333) following its individual manufacturer's instruction.

Immunoprecipitation

Cells were lysed in EBC lysis buffer supplemented with complete protease inhibitors (Roche Applied Bioscience). Lysates were clarified by centrifugation and then mixed with primary antibodies or 3F10 HA-conjugated beads (Roche Applied Bioscience) overnight.

For primary antibody incubation overnight, cell lysates were further incubated with protein G sepharose beads (Roche Applied Bioscience) for 2 h. Bound complexes were washed with NETN buffer eight times and were eluted by boiling in SDS loading buffer. Bound proteins were resolved in SDS-PAGE followed by western blot analysis.

Ubiquitination Assay

Cells were harvested and extracted in 100 μL of lysis buffer containing 1% SDS. Cell extracts were heat-denatured for 5 min and diluted with lysis buffer supplemented with complete protease inhibitors (Roche Applied Bioscience) and 20 mM N-ethylmaleimide (E3876, Sigma) to an SDS concentration of ≤0.1% (*36*). Diluted cell lysates were sonicated and clarified by centrifugation, followed by immunoprecipitation as described above. Immunoprecipitates were analyzed by immunoblotting with ubiquitin antibody (P4D1; sc-8017, Santa Cruz Biotechnology).

ChIP, ChIP-Seq, and Gene Expression Microarray Analysis

ChIP was performed with ZHX2 (Genetex, 112232) or p65 (Santa Cruz Biotechnology, sc-372-x) antibodies as previously described (*37, 38*). The ChIP-Seq library was prepared using a ChIP-Seq DNA sample preparation kit (Illumina) according to manufacturer's instructions. All ChIP-Seq peaks were identified using MACS package with a p-value cut-off of $1x10^{-5}$ (*39*). For gene expression microarray, total RNA was extracted using an RNeasy kit with on-column DNase digestion (Qiagen). Biotin-labeled cRNA was prepared from 500 ng of total RNA, fragmented, and hybridized to an Affymetrix human gene 2.0 ST expression array. All gene expression microarray data were normalized and summarized using RMA. Differentially expressed genes were identified using Limma. ChIP-PCR primers used in this study are listed below:

**ChIP Real-time PCR primers**

| | |
|---|---|
| IKBKE F | AGCCCCATCTCTCTTGGAGC |
| IKBKE R | CTCCCACACCACCACAAATC |
| ICAM1 F | CTCAGTTTCCCAGCGACAGG |
| ICAM1 R | GGAAGCTGCGTGATCCCTAC |
| IL8 F | TCTGACATAATGAAAAGATGAGGGT |
| IL8 R | CCTTCCGGTGGTTTCTTCCT |
| IL6 F | CGCTAGCCTCAATGACGACC |
| IL6 R | GGGTGGGGCTGATTGGAAAC |
| RNF207 F | AGTCCGATCCTTGCACCCTTG |
| RNF207 R | GCTCGCCATCTGCTTTGCG |
| ACTR3C F | CTCGCAGTTGGTACGTTCCTC |
| ACTR3C R | TCTCTAAGGCCGCACCGATA |
| LRRC37A3 F | GACCGCGCTCCGGTAAC |
| LRRC37A3 R | GGCTCAATCCGAATGGCTGG |

ChIP-seq Data Processing

ChIP and input control FASTQ files for ZHX2 and NF-κB–p65 were filtered requiring a quality score of ≥20 in at least 90% of nucleotides, and adapter contaminated reads were

removed with TagDust (*40*). Additionally, no more than five reads with identical sequences were retained. Non-filtered reads were aligned with GSNAP (*41*) to the hg19 human reference genome (parameter set: -k 15, -m 1). Post-alignment filtering was performed using blacklists created by ENCyclopedia Of DNA Elements (ENCODE) (*42*). Differentially enriched regions between ZHX2 and NF-κB–p65 or regions with common enrichment were then detected using MACS2 'bdgdiff', and ZHX2 replicates were combined by requiring both to exhibit a consistent pattern relative to NF-κB–p65. Enriched motifs among the top 1000 sites for each category were detected using HOMER (*43*). Motifs were discovered in the sequence underlying 50 bp upstream and downstream of peak summits (or midpoint of multiple summits, when applicable), compared to 100 bp of background sequence 1 kb upstream. ChIP-seq signal was normalized by the total number of aligned reads and plotted as the log2 ratio of ChIP/input control.

Integrative Analyses

Fold-changes of genes that were determined to be differentially expressed due to ZHX2 silencing (adj. $P < 0.05$) were compared to fold-changes due to NF-κB–p65 silencing. ChIP-seq signals were then plotted around the 5'-most transcriptional start site for each gene and further compared with ccRCC prognosis data. To evaluate prognostic value of each gene expression, we performed univariate Kaplan–Meier analysis using the Cox–Mantel log-rank test using software R (R package survival_2.40-1) (*44*). Patients were stratified into 2 or 3 equal-sized groups based on rank order of gene expression, and overall survival was used as an endpoint. We also performed univariate Cox proportional-hazards analysis of each gene individually. Prognostic value of genes was further characterized by calculating concordance index (C-index) using software R (R package Hmisc_4.0-1) (*45*). C-index is a measure of the probability that, given two randomly selected patients, the patient with the worse outcome is, in fact, predicted to have a worse outcome. This measure is similar to an area under the receiver operating characteristic curve, ranging 0.5–1.

GST Protein Purification and GST Pull Down

GST plasmids were transformed with BL21 competent cells. Single colonies were picked and cultured overnight in 50 mL of LB medium containing ampicillin. Then 5 mL of overnight cultures were diluted in 500 mL fresh LB medium and cultured with shaking at 37°C for 2–3 h, until OD600 reached 0.8–1.0. To induce GST production, 0.2 mM IPTG was added to cultures 4 h before harvesting pellets. Bacterial lysates were disrupted with a Nano DeBEE homogenizer (BEE International). Cleared bacterial lysates were purified using Glutathione-sepharose 4B beads. GST suspension proteins (20 μL) were incubated with either in vitro translated protein in 500 μL NETN buffer or cell lysates. After overnight incubation, bound complexes were washed with NETN buffer eight times, followed by boiling in SDS loading buffer and SDS-PAGE (*32*).

Real-Time PCR

Total RNA was isolated with an RNeasy mini kit (Qiagen). First strand cDNA was generated with an iScript cDNA synthesis kit (BioRad). Real-time PCR was performed in triplicate as previously described (*35*). Real-time PCR primers are listed below:

**mRNA Real-time PCR primers**

| | |
|---|---|
| ZHX2 F | GATCAGATAGCTGGAGTCAGGC |

| | |
|---|---|
| ZHX2 R | CACAGCAGTTCTAACAGACTTCC |
| VHL F | GACACACGATGGGCTTCTGGTT |
| VHL R | ACAACCTGGAGGCATCGCTCTT |
| CCL2 F | AGAATCACCAGCAGCAAGTGTCC |
| CCL2 R | TCCTGAACCCACTTCTGCTTGG |
| IL8 F | GAGAGTGATTGAGAGTGGACCAC |
| IL8 R | CACAACCCTCTGCACCCAGTTT |
| ICAM1 F | AGCGGCTGACGTGTGCAGTAAT |
| ICAM1 R | TCTGAGACCTCTGGCTTCGTCA |
| IL6 F | AGACAGCCACTCACCTCTTCAG |
| IL6 R | TTCTGCCAGTGCCTCTTTGCTG |
| VCAM1 F | GATTCTGTGCCCACAGTAAGGC |
| VCAM1 R | TGGTCACAGAGCCACCTTCTTG |
| BCL2 F | ATCGCCCTGTGGATGACTGAGT |
| BCL2 R | GCCAGGAGAAATCAAACAGAGGC |
| TNF F | CTCTTCTGCCTGCTGCACTTTG |
| TNF R | ATGGGCTACAGGCTTGTCACTC |
| B-Actin F | AGAAAATCTGGCACCACACC |
| B-Actin R | GGGGTGTTGAAGGTCTCAAA |

Cell Proliferation Assays

Cells were plated in triplicate in 96-well plates (1000 cells/well) in appropriate growth medium. At indicated time points, cells were replaced with 90 μL fresh growth medium supplemented with 10 μL MTS reagents (Promega), followed by incubation at 37°C for 1 h. OD absorbance values were measured at 490 nm using a 96-well plate reader (Tecan).

Anchorage-Independent Growth Assays

Cells were plated at a density of 5000 cells/mL for 786-O cells and 2500 cells/mL for UMRC2 or UMRC6 cells in complete medium with 0.4% agarose onto bottom layers composed of medium with 1% agarose. Cells were incubated at 4ºC for 10 min and then placed in a 37ºC incubator. Every 4 d, three drops of complete media were added onto the plate. After incubating 786-O cells for four weeks or UMRC2 or UMRC6 cells for two weeks, extra liquid on the plate was aspirated and 1 mL of medium was added to each well. Colonies were stained with 100 μg/mL iodonitrotetrazoliuim chloride solution. Cell culture plates were incubated overnight and foci numbers were counted.

Orthotopic Tumor Growth

Six-week old female NOD SCID Gamma mice (NSG, Jackson Lab) were used for xenograft studies. Approximately $5\times10^5$ viable 786-O kidney cancer cells were resuspended in 20 μL fresh growth medium and injected orthotopically into the left kidney of each mouse as described previously (*46*). Bioluminescence imaging was performed as described previously (*35, 47*). For non-inducible ZHX2 shRNA, mice were euthanized 7 weeks after the first imaging. For inducible Teton-ZHX2 shRNA, after injection and following 3 consecutive weeks of bioluminescence imaging to make sure tumors were successfully implanted in the kidney, mice were fed Purina rodent chow with doxycycline

(#5001, Research Diets Inc.). Mice were euthanized 6 weeks after treatment with doxycycline. Rough mass of tumors is presented as mean ± SEM. All animal experiments were in compliance with National Institutes of Health guidelines and were approved by the University of North Carolina at Chapel Hill Animal Care and Use Committee.

Human ccRCC tumors

Fresh-frozen samples or paraffin-embedded samples of ccRCC and their accordingly adjacent normal tissues were obtained from tissue procurement facility at UNC. All human tumor sample related studies have been approved by the University of North Carolina at Chapel Hill Institutional Review Board (IRB). Genetically defined ccRCC patient tissues with loss of VHL or WT VHL were obtained from UNCseq projects (*48*). Paraffin-embeded samples of ccRCC TMA slides were obtained from MD Anderson Cancer Center (*49*), immunohistochemically stained with ZHX2 antibody. Calculation of cytoplasmic and nuclear staining scores were performed by a previously described algorithm (*50*).

Tumor sample sequencing

Total genome DNA was isolated with an AllPrep DNA/RNA mini kit (Qiagen) followed by library prep using the Agilent SureSelect kit for targeted exome with the UNCSeq capture (bait version v.10). All 10 tumor samples were pooled into one pool and then sequenced on the NextSeq500 using a 300 cycle High Output kit (*51*).

Cell line block preparation using low melting agarose

Cells were washed gently with sterile 1xPBS and treated with trypsin followed by adding 3-5 ml media to inactivate trypsin. Cell pellet was washed with 1xPBS twice followed by fixation with 10% neutral-buffered formalin (NBF) overnight. Cell pellet was resuspended in small volume of 80% ethanol followed by 60°C incubation. Subsequently, cell clot was prepared for mold. Briefly, plastic transfer pipette was cut to 1 cm tubes, which will be used as a mold. 3% low melting agarose was added on microscope slide, prepared molds were added on the top of agarose drop and bottom of the tube was pressed followed by agarose hardening for 1-2 min. Cell pellet was resuspended in equal volume of agarose (pellet size: agarose=1:1) and was transferred to the prepared mold and molds were into refrigerator for 5-10 min. When agarose-cell clot was hardened, it was pushed from mold with clean transfer pipette into micromesh cassette. Cassettes were submerged in 80% ethanol overnight for further immunohistochemistry staining.

Immunohistochemistry Staining

Formalin-fixed paraffin-embedded (FFPE) tissue sections were immunostained in a Bond automated slide staining system (Leica Microsystems). Slides were dewaxed in Bond dewax solution (AR9222) and hydrated. Heat-induced antigen retrieval was performed for 30 min in Bond-Epitope Retrieval Solution 1 pH 6.8 (citrate buffer). Antigen retrieval was followed with 5 min Bond peroxide blocking (DS9800) and 10 min Bond protein blocking (PV6122) steps. After pretreatment, tissues were incubated with 1:100 rabbit polyclonal anti-ZHX2 antibody (GeneTex, GTX112232) or 1:100 HIF2α rabbit antibody (Novus, NB100-122) for 1 h. Detection was performed using Bond Polymer Refine Detection System (DS9800). Stained slides were dehydrated and cover-slipped.

Semi-quantitative analysis

A tissue microarray was constructed using FFPE tissue from hysterectomy specimens as described previously (*49*). Tissue array sections were immunostained with a commercially available ZHX2 antibody (Catalogue No 112232, Genetex). Tissue microarray cores were examined and scored by a light microscope at a power of 400X, most of them have triplicates, some do not. We interpreted cytoplasmic and nuclear staining separately, as well as collectively. We also considered staining intensity and area extent using the German semi-quantitative scoring system, which has been widely accepted and used in previous studies (*50*). Every tumor was given a score according to intensity of nuclear or cytoplasmic staining (no staining = 0; weak staining = 1; moderate staining = 2; strong staining = 3) and percentage of tumor cells with positive ZHX2 staining (0% = 0; 1–10% = 1; 11–50% = 2; 51–80% = 3; 81–100% = 4).

Statistical Analysis

Unpaired two-tailed student's *t*-test was used for experiments comparing two sets of data. Data represent mean ± SEM from three independent experiments. *, **, and *** denote p value of <0.05, 0.01, and 0.005, respectively. NS denotes not significant.

**Figure S1**

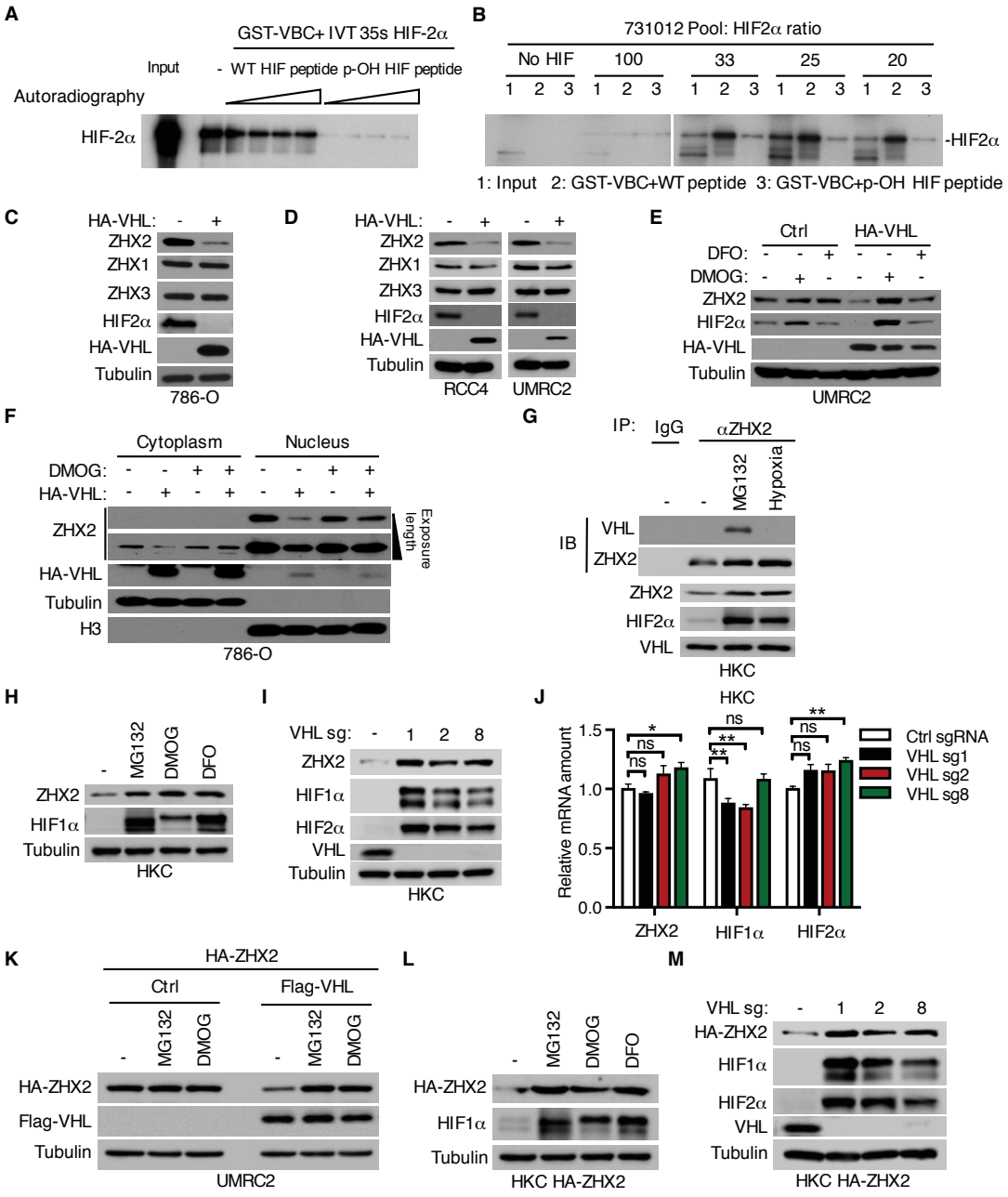
A
GST-VBC+ IVT 35s HIF-2α
Input
- WT HIF peptide p-OH HIF peptide
Autoradiography
HIF-2α
B
731012 Pool: HIF2α ratio
No HIF
100
33
25
20
1 2 3 1 2 3 1 2 3 1 2 3 1 2 3
-HIF2α
1: Input 2: GST-VBC+WT peptide 3: GST-VBC+p-OH HIF peptide
C
HA-VHL: - +
ZHX2
ZHX1
ZHX3
HIF2α
HA-VHL
Tubulin
786-O
D
HA-VHL: - + - +
ZHX2
ZHX1
ZHX3
HIF2α
HA-VHL
Tubulin
RCC4
UMRC2
E
Ctrl
HA-VHL
DFO: - - + - - +
DMOG: - + - - + -
ZHX2
HIF2α
HA-VHL
Tubulin
UMRC2
F
Cytoplasm
Nucleus
DMOG: - - + + - - + +
HA-VHL: - + - + - + - +
ZHX2
Exposure length
HA-VHL
Tubulin
H3
786-O
G
IP: IgG
αZHX2
MG132
Hypoxia
- - + +
IB
VHL
ZHX2
ZHX2
HIF2α
VHL
HKC
H
MG132
DMOG
DFO
-
ZHX2
HIF1α
Tubulin
HKC
I
VHL sg: - 1 2 8
ZHX2
HIF1α
HIF2α
VHL
Tubulin
HKC
J
HKC
Relative mRNA amount
1.5
1.0
0.5
0.0
*
ns
**
ns
**
ns
**
ns
Ctrl sgRNA
VHL sg1
VHL sg2
VHL sg8
ZHX2
HIF1α
HIF2α
K
HA-ZHX2
Ctrl
Flag-VHL
MG132
DMOG
MG132
DMOG
-
HA-ZHX2
Flag-VHL
Tubulin
UMRC2
L
MG132
DMOG
DFO
-
HA-ZHX2
HIF1α
Tubulin
HKC HA-ZHX2
M
VHL sg: - 1 2 8
HA-ZHX2
HIF1α
HIF2α
VHL
Tubulin
HKC HA-ZHX2

**Figure S1. Validation of the screening strategy and ZHX2 regulation by VHL through prolyl hydroxylation and proteasomal degradation.**

**(A)** Binding competition assay with in vitro translated HIF2α to validate the VHL substrate screening strategy.

**(B)** Binding competition assays with HIF2α at various ratios of cDNA pool/HIF2α to further validate the screening strategy.

**(C)** Immunoblots of lysates with indicated antibodies from 786-O cells infected with lentivirus encoding either control vector or HA-VHL.

**(D)** Immunoblots of lysates from RCC4 or UMRC2 cells infected with lentivirus encoding either control vector or HA-VHL.

**(E)** Immunoblots of lysates from UMRC2 cells infected with lentivirus encoding either control vector (Ctrl) or HA-VHL and treated as indicated for 8 h.

**(F)** Immunoblots of cell fractions of 786-O cells infected with lentivirus encoding either control vector or HA-VHL and treated with as indicated for 8 h.

**(G)** Immunoblots (IB) of whole cell extracts (WCE) and immunoprecipitations (IP) of HKC cells with indicated treatments for 8 h.

**(H)** Immunoblots of lysates from HKC cells treated with indicated inhibitors for 8 h.

**(I–J)** Immunoblot of cell lysates (I) and qRT-PCR quantification of mRNA (J) from HKC cells infected with lentivirus encoding either VHL sgRNAs (1, 2, or 8) or control (Ctrl) sgRNA (mean ± SEM, n=3 replicates per group, unpaired *t*-test). * and ** denote p value of <0.05 and <0.01, respectively, ns denotes not significant.

**(K)** Immunoblots of lysates from UMRC2 cells transfected with indicated plasmids and treated with indicated inhibitors for 8 h.

**(L)** Immunoblots of lysates from HKC cells infected with lentivirus encoding HA-ZHX2 and treated with indicated inhibitors for 8 h.

**(M)** Immunoblot of cell lysates from HKC cells infected with lentivirus encoding HA-ZHX2, followed by another infection with lentivirus encoding either VHL sgRNAs (1, 2, or 8) or control (Ctrl) sgRNA.

## Figure S2

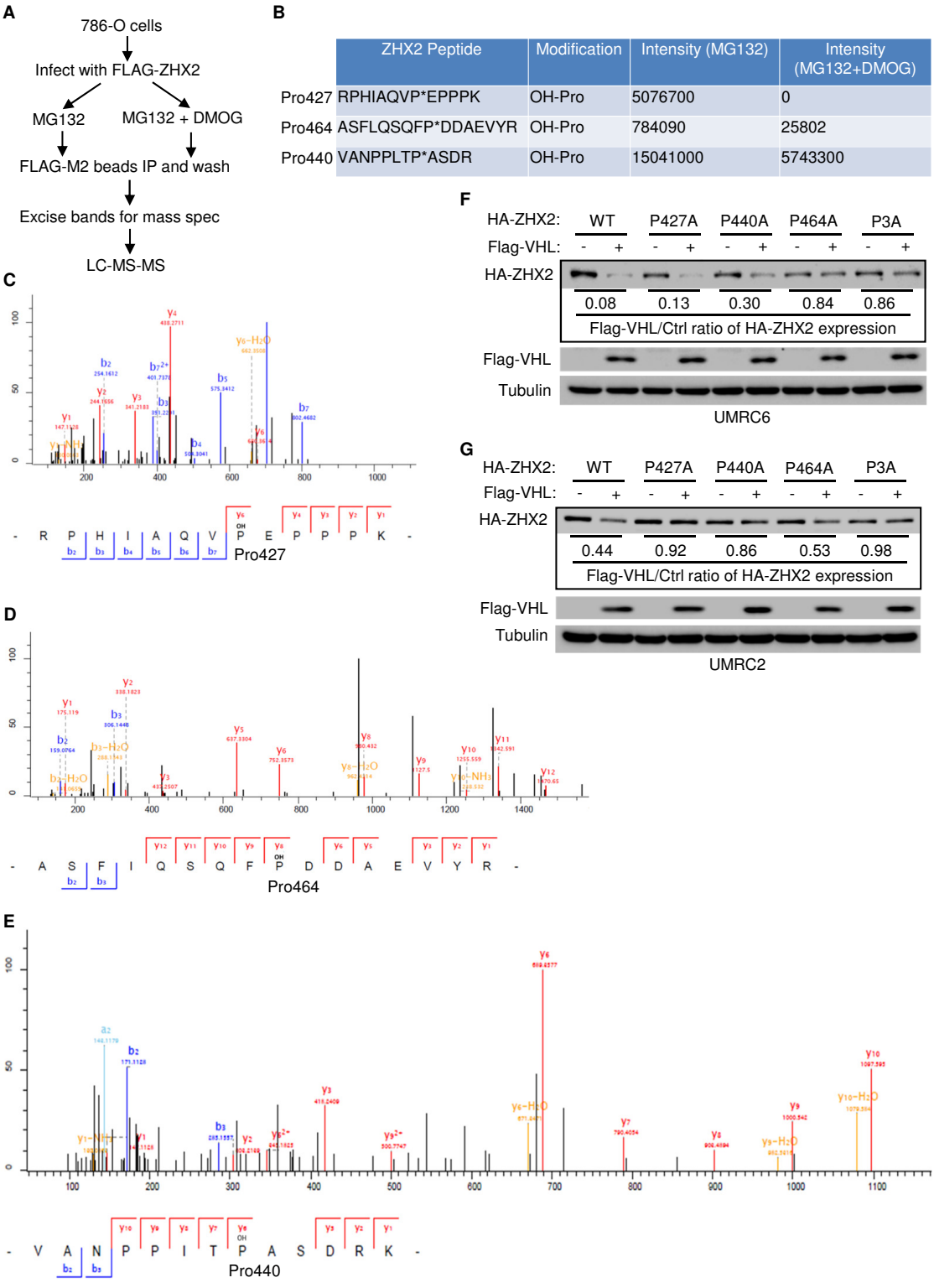
A
786-O cells
Infect with FLAG-ZHX2
MG132
MG132 + DMOG
FLAG-M2 beads IP and wash
Excise bands for mass spec
LC-MS-MS
B
ZHX2 Peptide | Modification | Intensity (MG132) | Intensity (MG132+DMOG)
Pro427 RPHIAQVP*EPPPK | OH-Pro | 5076700 | 0
Pro464 ASFLQSQFP*DDAEVYR | OH-Pro | 784090 | 25802
Pro440 VANPPLTP*ASDR | OH-Pro | 15041000 | 5743300
C
Pro427
D
Pro464
E
Pro440
F
HA-ZHX2: WT P427A P440A P464A P3A
Flag-VHL: - + - + - + - + - +
HA-ZHX2
0.08 0.13 0.30 0.84 0.86
Flag-VHL/Ctrl ratio of HA-ZHX2 expression
Flag-VHL
Tubulin
UMRC6
G
HA-ZHX2: WT P427A P440A P464A P3A
Flag-VHL: - + - + - + - + - +
HA-ZHX2
0.44 0.92 0.86 0.53 0.98
Flag-VHL/Ctrl ratio of HA-ZHX2 expression
Flag-VHL
Tubulin
UMRC2

**Figure S2. Mass spectrometry identifies three ZHX2 prolyl hydroxylation sites which mediate ZHX2 stability regulated by VHL.**
**(A)** Schematic representation of ZHX2 prolyl hydroxylation identification strategy by mass spectrometry.
**(B)** Intensity values of three potential prolyl hydroxylation sites identified in mass spectrometry analysis.
**(C–E)** MS/MS spectrum for identified hydroxylated ZHX2 peptides at Pro427 (C), Pro440 (D), and Pro464 (E).
**(F–G)** Immunoblots of lysates from UMRC6 (F) or UMRC2 (G) cells transfected with indicated plasmids followed by densitometry analysis for HA-ZHX2 blots with ImageJ.

**Figure S3**

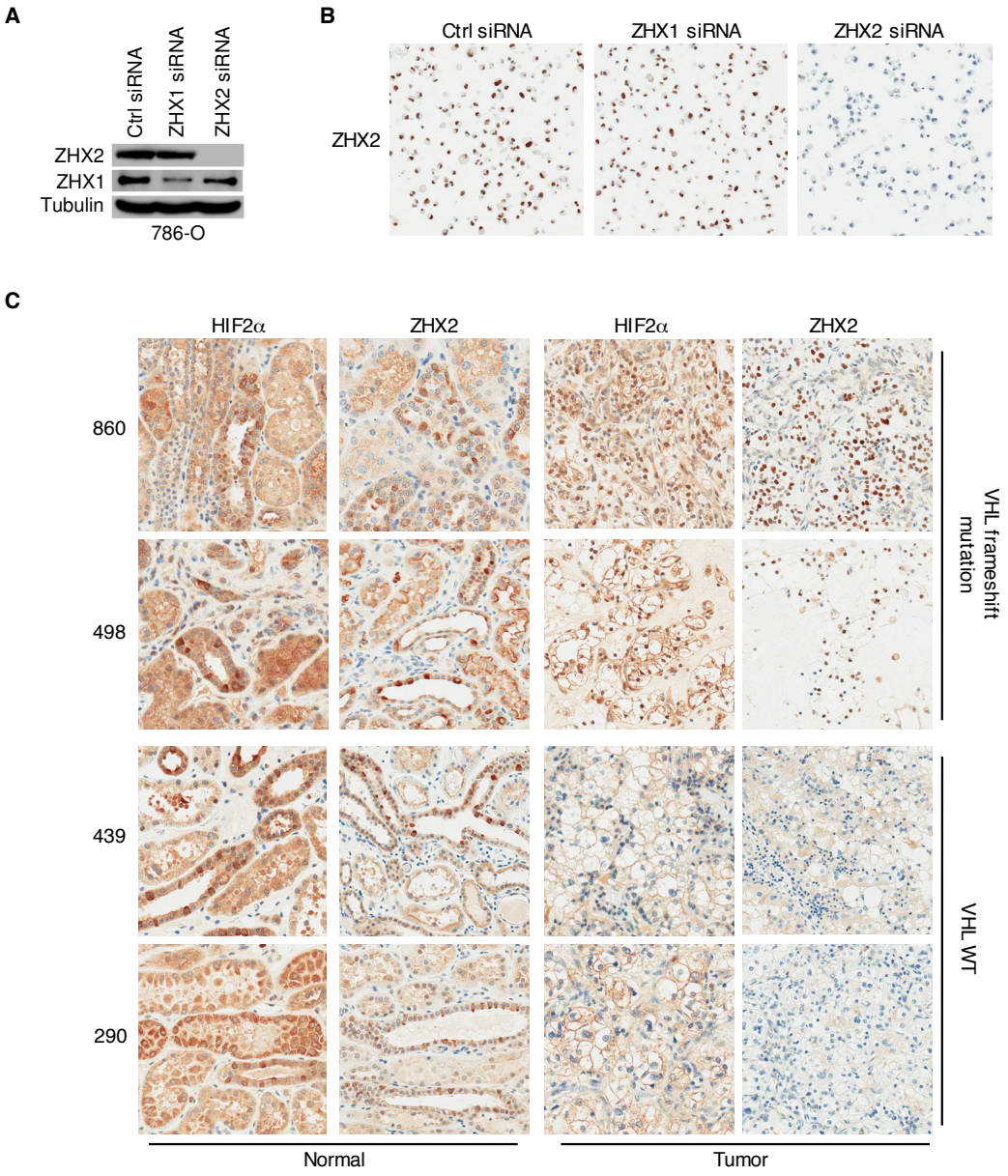


**Figure S3. ZHX2 antibody verification.**

**(A-B)** ZHX2 antibody specifically recognized ZHX2 but not ZHX1. Immunoblots (A) and immunohistochemistry staining (B) of 786-O cells transfected with either ZHX2 siRNA, ZHX1 siRNA or control (Ctrl) siRNA.

**(C)** Representative ZHX2 or HIF2α immunohistochemistry staining for indicated ccRCC patient tissues.

## Figure S4

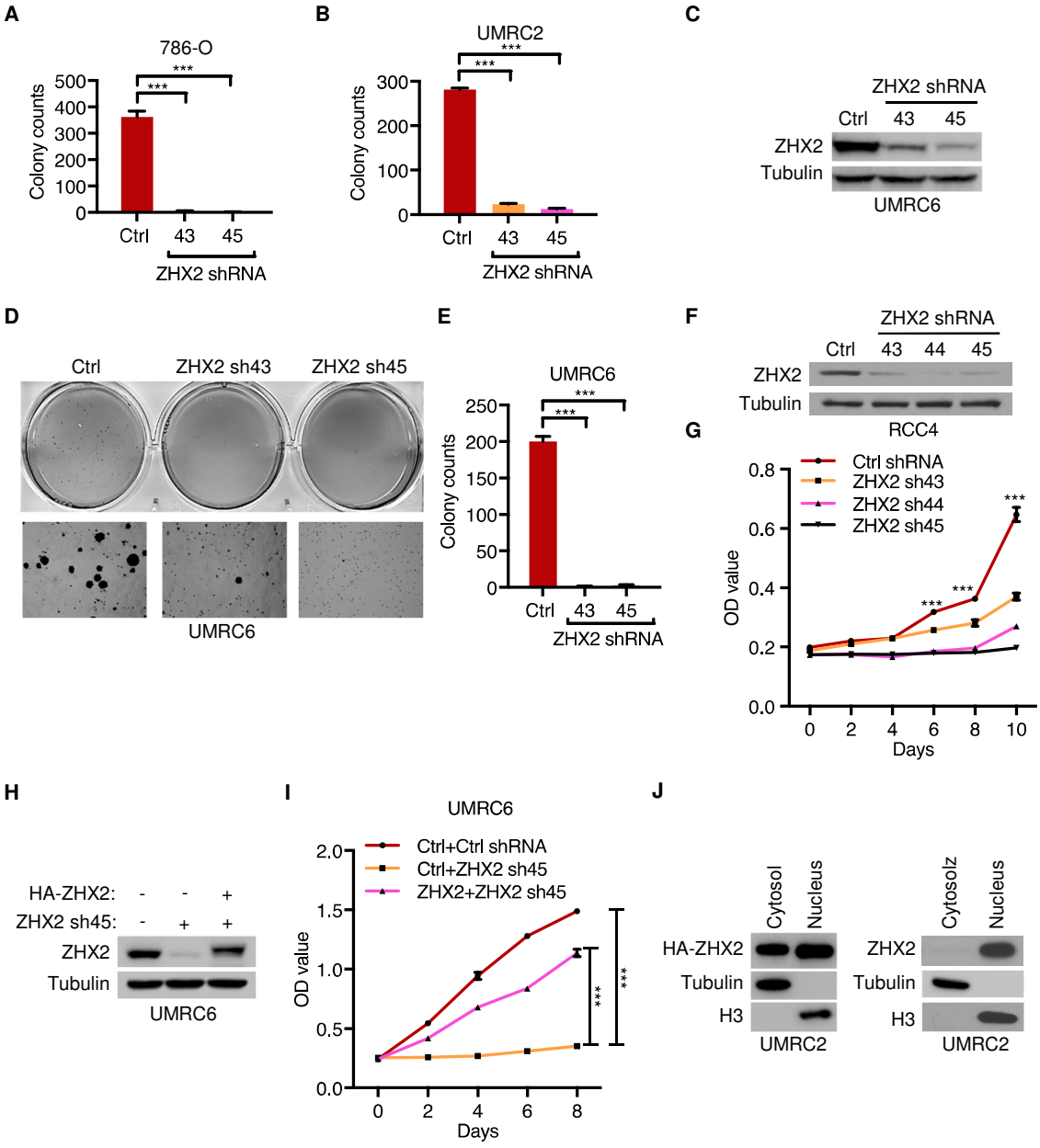
A
786-O
Colony counts
500
400
300
200
100
0
***
***
Ctrl
43
45
ZHX2 shRNA
B
UMRC2
Colony counts
300
200
100
0
***
***
Ctrl
43
45
ZHX2 shRNA
C
ZHX2 shRNA
Ctrl
43
45
ZHX2
Tubulin
UMRC6
D
Ctrl
ZHX2 sh43
ZHX2 sh45
UMRC6
E
UMRC6
Colony counts
250
200
150
100
50
0
***
***
Ctrl
43
45
ZHX2 shRNA
F
ZHX2 shRNA
Ctrl
43
44
45
ZHX2
Tubulin
RCC4
G
Ctrl shRNA
ZHX2 sh43
ZHX2 sh44
ZHX2 sh45
OD value
0.8
0.6
0.4
0.2
0.0
0
2
4
6
8
10
Days
***
***
***
H
HA-ZHX2:
ZHX2 sh45:
ZHX2
Tubulin
UMRC6
I
UMRC6
Ctrl+Ctrl shRNA
Ctrl+ZHX2 sh45
ZHX2+ZHX2 sh45
OD value
2.0
1.5
1.0
0.5
0.0
0
2
4
6
8
Days
***
***
J
Cytosol
Nucleus
HA-ZHX2
Tubulin
H3
UMRC2
Cytosolz
Nucleus
ZHX2
Tubulin
H3
UMRC2

**Figure S4. ZHX2 depletion by shRNAs decreases ccRCC cell proliferation and anchorage-independent growth.**

**(A–B)** Quantification of soft agar assays for 786-O (A) and UMRC2 (B) cells from main figure 3e and 3f.

**(C-E)** Immunoblots of cell lysates (C) and representative anchorage-independent growth assays (D) and their quantification (E) of UMRC6 cells infected with lentivirus encoding either ZHX2 shRNAs (43, 45) or control (Ctrl) shRNA.

**(F-G)** Immunoblots of cell lysates (F) and cell proliferation assays (G) of RCC4 cells infected with lentivirus encoding either ZHX2 shRNAs (43, 44, 45) or control (Ctrl) shRNA.

**(H-I)** Immunoblots of cell lysates (H) and cell proliferation assays (I) of UMRC6 cells transfected with ZHX2 sh45-resistant HA-ZHX2 or control (Ctrl) vector, followed by infection with lentivirus encoding either ZHX2 sh45 or control (Ctrl) shRNA.

**(J)** Immunoblots of lysates from cell fractions of UMRC2 cells infected with lentivirus encoding HA-ZHX2 or UMRC2 parental cells.

Error bars represent mean ± SEM, n=3 replicates per group, unpaired *t*-test. *** denotes p value of <0.005.

**Figure S5**

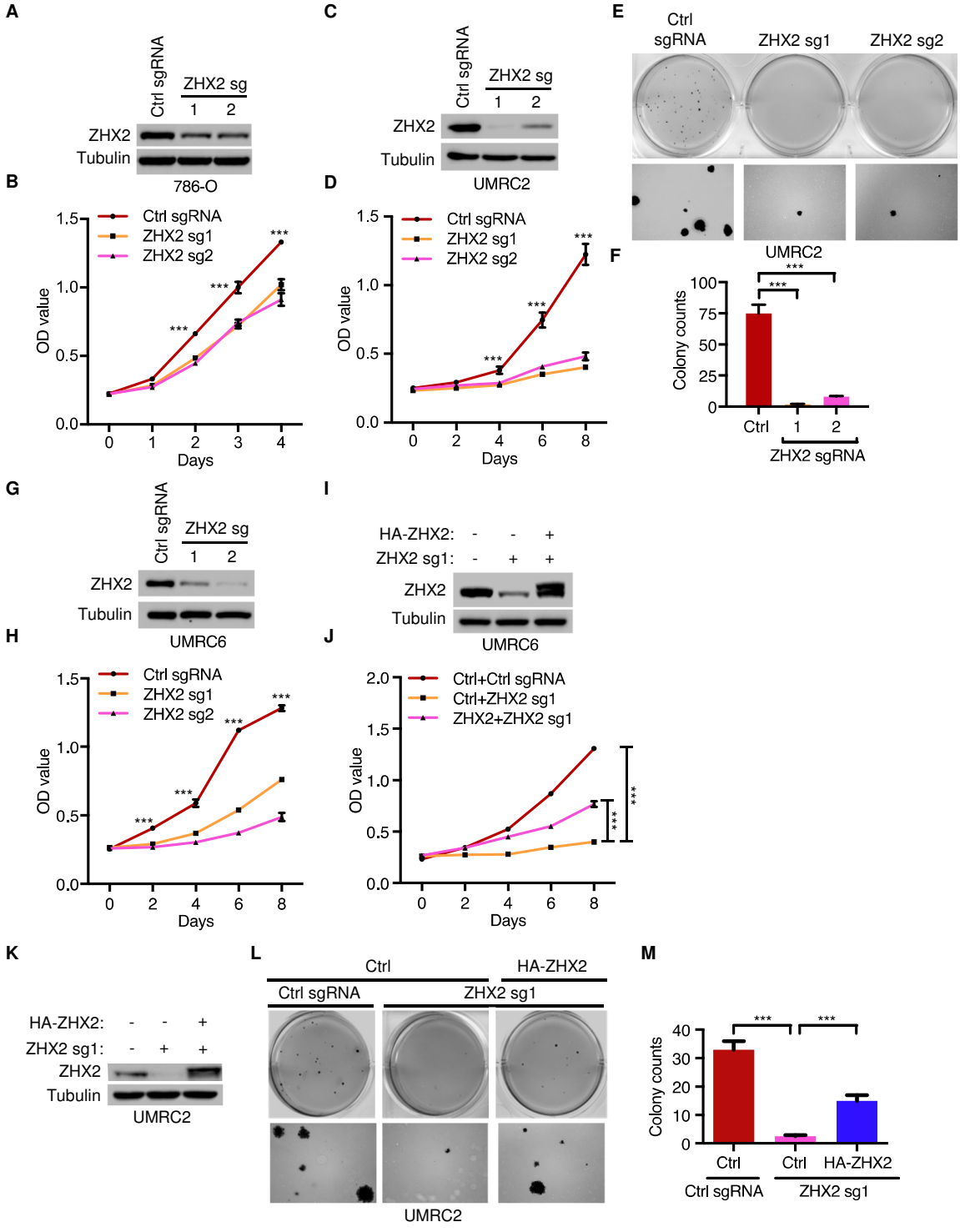
A
Ctrl sgRNA
ZHX2 sg
1
2
ZHX2
Tubulin
786-O
B
Ctrl sgRNA
ZHX2 sg1
ZHX2 sg2
OD value
Days
C
UMRC2
D
E
Ctrl sgRNA
ZHX2 sg1
ZHX2 sg2
UMRC2
F
Colony counts
Ctrl
ZHX2 sgRNA
G
H
I
HA-ZHX2:
ZHX2 sg1:
UMRC6
J
Ctrl+Ctrl sgRNA
Ctrl+ZHX2 sg1
ZHX2+ZHX2 sg1
K
L
Ctrl
HA-ZHX2
M

**Figure S5. CRISPR-Cas9 mediated ZHX2 depletion leads to decreased ccRCC cell proliferation and anchorage-independent growth.**

**(A–B)** Immunoblots of cell lysates (A) and quantification of cell proliferation assays (B) of 786-O cells infected with lentivirus encoding either control (Ctrl) shRNA or ZHX2 sgRNAs (1, 2) or control (Ctrl) sgRNA.

**(C–F)** Immunoblots of cell lysates (C), quantification of cell proliferation assays (D), and representative cell invasion assays (E) and their quantification (F) of UMRC2 cells infected with lentivirus encoding ZHX2 sgRNAs (1, 2) or control (Ctrl) sgRNA.

**(G–H)** Immunoblots of cell lysates (G) and quantification of cell proliferation assays (H) of UMRC6 cells infected with lentivirus encoding ZHX2 sgRNAs (1, 2) or control (Ctrl) sgRNA.

**(I-J)** Immunoblots of cell lysates (I) and cell proliferation assays (J) of UMRC6 cells transfected with ZHX2 sg1-resistant HA-ZHX2 or control (Ctrl) vector, followed by infection with lentivirus encoding either ZHX2 sg1 or control (Ctrl) sgRNA.

**(K–M)** Immunoblots of cell lysates (K) and representative anchorage-independent growth assays (L) and their quantification (M) of UMRC2 cells transfected with ZHX2 sg1-resistant HA-ZHX2 or control (Ctrl) vector, followed by infection with lentivirus encoding either ZHX2 sg1 or control (Ctrl) sgRNA.

Error bars represent mean ± SEM, n=3 replicates per group, unpaired *t*-test. *** denotes p value of <0.005.

**Figure S6**

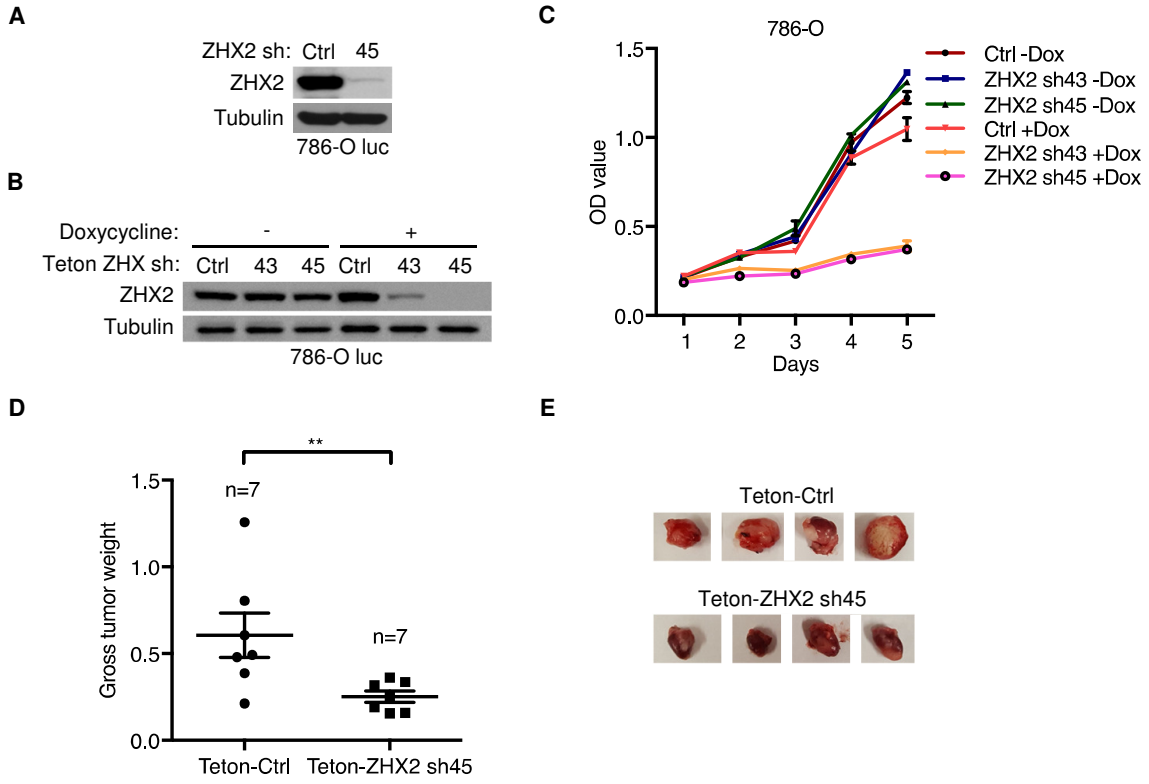


**Figure S6. ZHX2 contributes to ccRCC tumorigenesis and maintenance.**
**(A)** Immunoblot of cell lysates of 786-O luciferase cell lines infected with lentivirus encoding either ZHX2 shRNA (45) or control (Ctrl).
**(B-C)** Immunoblots of cell lysates (B) and cell proliferation assays (C) of 786-O luciferase stable cells infected with lentivirus encoding either Teton-ZHX2 shRNAs (43, 45) or Teton control (Ctrl) shRNA and treated with or without doxycycline as indicated (Error bars represent mean ± SEM, n=3 replicates per group).
**(D-E)** Plot of gross tumor weights (D) and representative gross tumors (E) (including kidney and tumor tissue) at necropsy of mice injected with cells infected with lentivirus encoding either Teton-ZHX2 sh45 or Teton-control (Teton-Ctrl) shRNA.
Error bars represent mean ± SEM, unpaired *t*-test. ** denotes p value of <0.01.

**Figure S7**

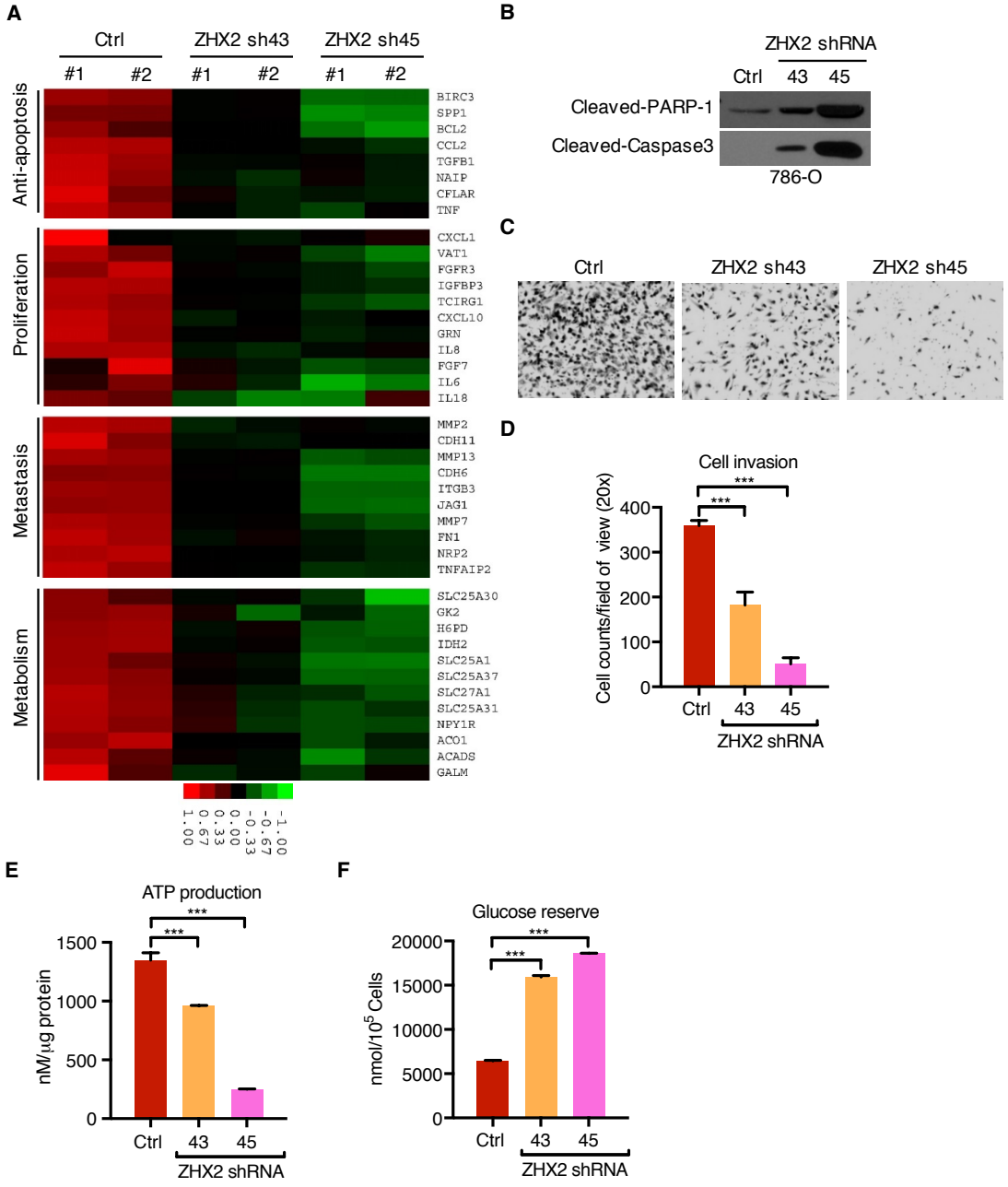
A
Ctrl
ZHX2 sh43
ZHX2 sh45
#1
#2
#1
#2
#1
#2
Anti-apoptosis
BIRC3
SPP1
BCL2
CCL2
TGFB1
NAIP
CFLAR
TNF
Proliferation
CXCL1
VAT1
FGFR3
IGFBP3
TCIRG1
CXCL10
GRN
IL8
FGF7
IL6
IL18
Metastasis
MMP2
CDH11
MMP13
CDH6
ITGB3
JAG1
MMP7
FN1
NRP2
TNFAIP2
Metabolism
SLC25A30
GK2
H6PD
IDH2
SLC25A1
SLC25A37
SLC27A1
SLC25A31
NPY1R
ACO1
ACADS
GALM
1.00
0.67
0.33
0.00
-0.33
-0.67
-1.00
B
ZHX2 shRNA
Ctrl
43
45
Cleaved-PARP-1
Cleaved-Caspase3
786-O
C
Ctrl
ZHX2 sh43
ZHX2 sh45
D
Cell invasion
Cell counts/field of view (20x)
400
300
200
100
0
***
***
Ctrl
43
45
ZHX2 shRNA
E
ATP production
nM/μg protein
1500
1000
500
0
***
***
Ctrl
43
45
ZHX2 shRNA
F
Glucose reserve
nmol/10^5 Cells
20000
15000
10000
5000
0
***
***
Ctrl
43
45
ZHX2 shRNA

**Figure S7. ZHX2 regulates various oncogenic pathways.**
**(A)** Heat map of expression microarray analysis of genes involved in anti-apoptosis, proliferation, metastasis, and metabolism upon ZHX2 depletion in 786-O cells, from GSEA through DAVID Bioinformatics Resources (*52*).
**(B–F)** Immunoblots of cell lysates (B) (immunoblots for ZHX2 and Tubulin were shown in Fig 3A), representative invaded cell images (C), quantification of cell invasion assays (D), quantification of ATP production assays (E), and quantification of glucose reserve assays (F) of 786-O cells infected with lentivirus encoding either ZHX2 shRNAs (43, 45) or control (Ctrl) shRNA. Error bars represent mean ± SEM, n=3 replicates per group, unpaired *t*-test. *** denotes p value of <0.005.

**Figure S8**

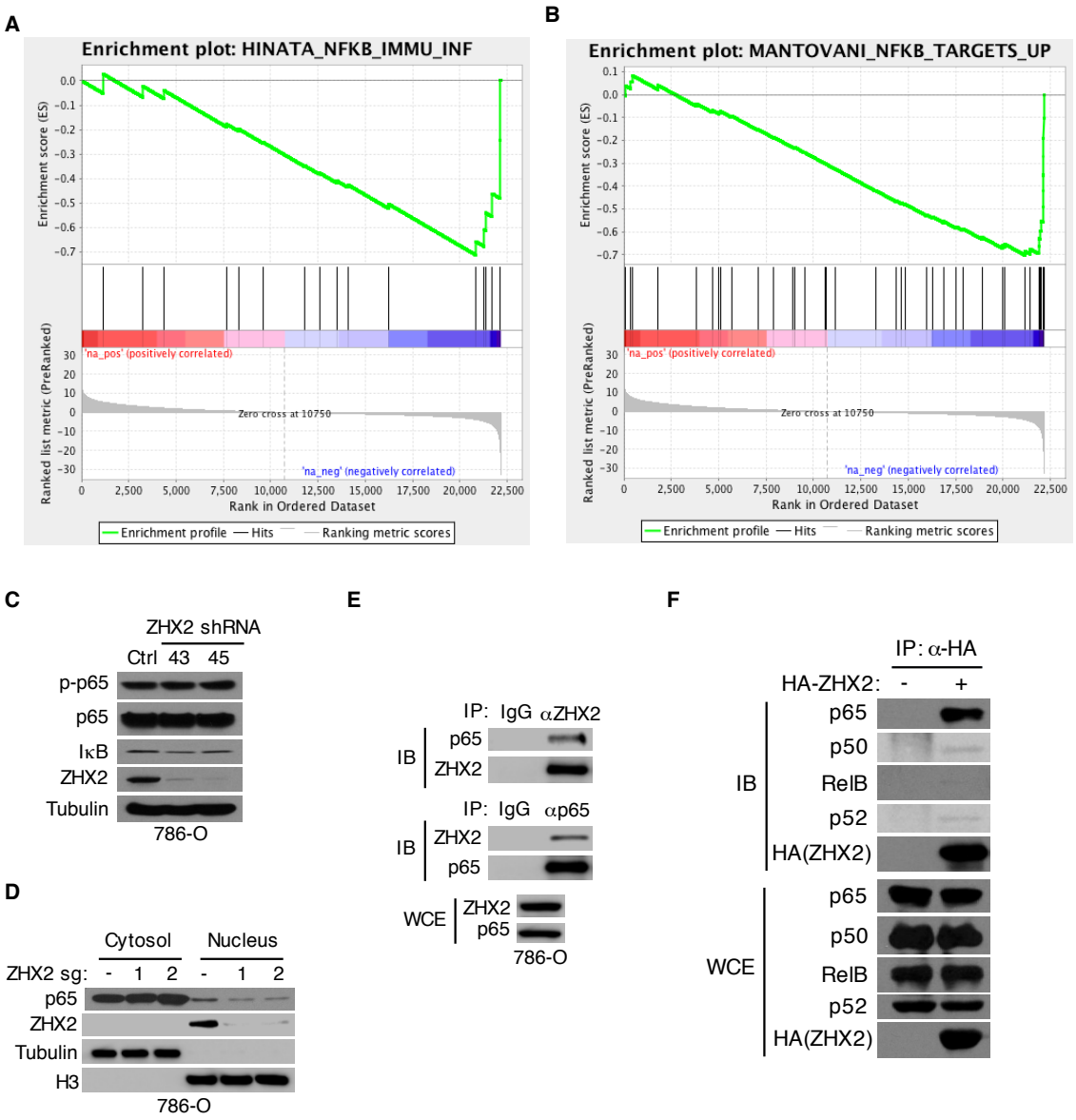


**Figure S8. ZHX2 regulates NF-κB activation.**

**(A–B)** GSEA histograms for gene sets representing NF-κB signaling downstream target genes.

**(C)** Immunoblots of cell fractions from 786-O cells infected with lentivirus encoding either ZHX2 shRNAs (43, 45) or control shRNA.

**(D)** Immunoblots of cell lysates from 786-O cells infected with lentivirus encoding either ZHX2 sgRNAs (1, 2) or control (Ctrl) sgRNA.

**(E)** Immunoblots (IB) of whole cell extracts (WCE) and immunoprecipitations (IP) of 786-O cells with indicated antibodies.

**(F)** Immunoblots (IB) of whole cell extract (WCE) and immunoprecipitations (IP) of 293T cells transfected with indicated plasmids.

## Figure S9

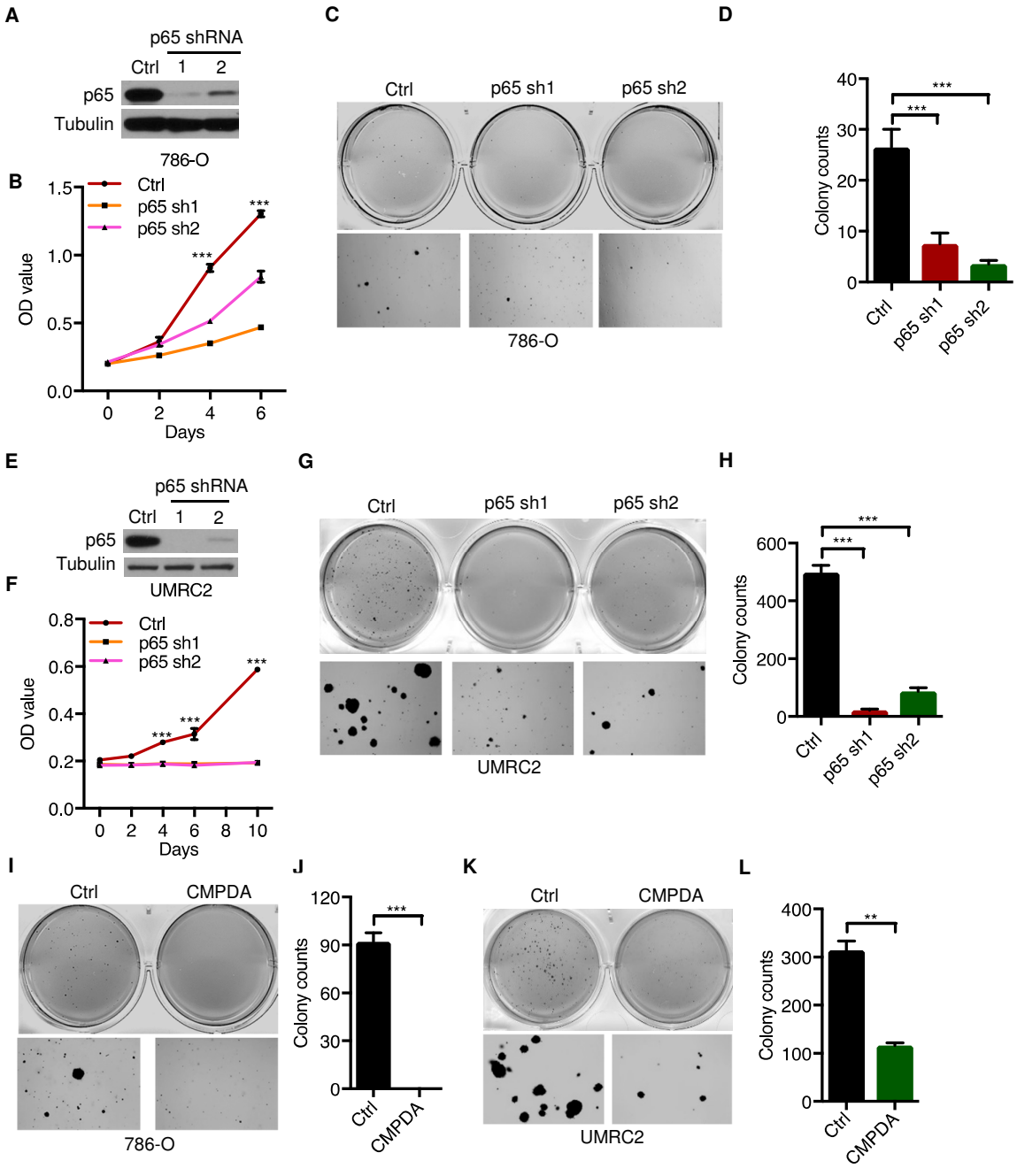
A
p65 shRNA
Ctrl 1 2
p65
Tubulin
786-O
B
Ctrl
p65 sh1
p65 sh2
OD value
Days
C
Ctrl
p65 sh1
p65 sh2
786-O
D
Colony counts
Ctrl
p65 sh1
p65 sh2
E
p65 shRNA
Ctrl 1 2
p65
Tubulin
UMRC2
F
Ctrl
p65 sh1
p65 sh2
OD value
Days
G
Ctrl
p65 sh1
p65 sh2
UMRC2
H
Colony counts
Ctrl
p65 sh1
p65 sh2
I
Ctrl
CMPDA
786-O
J
Colony counts
Ctrl
CMPDA
K
Ctrl
CMPDA
UMRC2
L
Colony counts
Ctrl
CMPDA

**Figure S9. NF-κB activity contributes to ccRCC.**
**(A–D)** Immunoblots of cell lysates (A), quantification of cell proliferation assays (B), and representative anchorage-independent growth assays (C) and their quantification (D) from 786-O cells infected with lentivirus encoding either p65 shRNAs (1, 2) or control (Ctrl) shRNA.
**(E-H)** Immunoblots of cell lysates (E), cell proliferation assays (F), representative anchorage-independent growth assays (G), and their quantification (H) from UMRC2 cells infected with lentivirus encoding either p65 shRNAs (1, 2) or control (Ctrl) shRNA.
**(I–J)** Representative anchorage-independent growth assays (I) and their quantification (J) from control 786-O cells (Ctrl) or cells treated with CMPDA (5 μM) as indicated.
**(K-L)** Representative anchorage-independent growth assays (K) and their quantification (L) from control UMRC2 cells (Ctrl) or cells treated with CMPDA (5 μM) daily as indicated.
Error bars represent mean ± SEM, n=3 replicates per group, unpaired *t*-test. ** and *** denotes p value of <0.01 and <0.005, respectively.

**Figure S10**

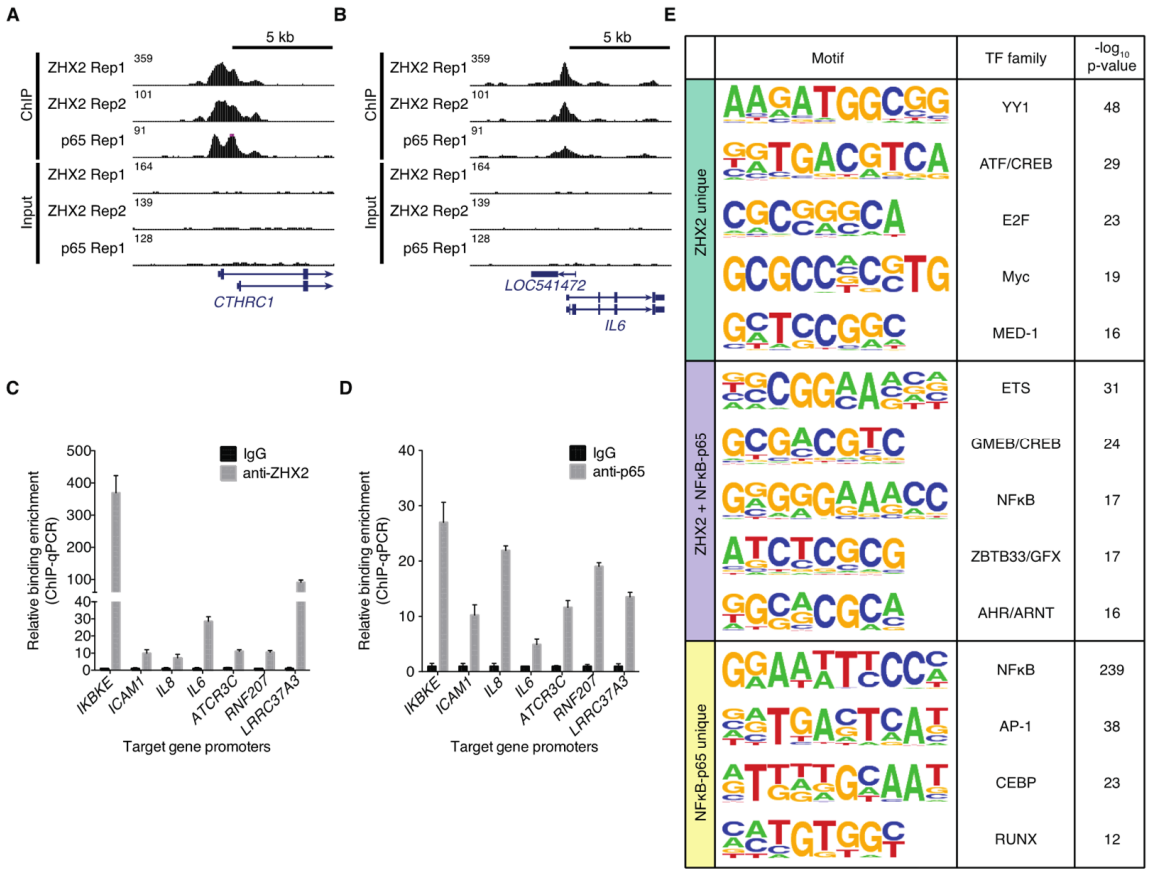


**Figure S10. Representative ZHX2 and NF-κB–p65 downstream targets and analysis of their chromatin binding motifs.**

**(A–B)** UCSC Genome Browser snapshots of four loci with common ChIP-seq enrichment between ZHX2 and NF-κB–p65. Data are scaled to be proportional to aligned read depth.

**(C–D)** ChIP-qPCR validation of binding for ZHX2 (C) and NF-κB–p65 (D) at seven target gene promoters compared to IgG control. Error bars represent mean ± SEM of three replicates.

**(E)** Over-enriched transcription factor motifs for sites unique to ZHX2 (green), common between ZHX2 and NF-κB–p65 (purple), and unique to NF-κB–p65 (yellow). The general family of transcription factors is shown alongside the -log10 of p-value of enrichment compared to nearby background sequence.

**Figure S11**

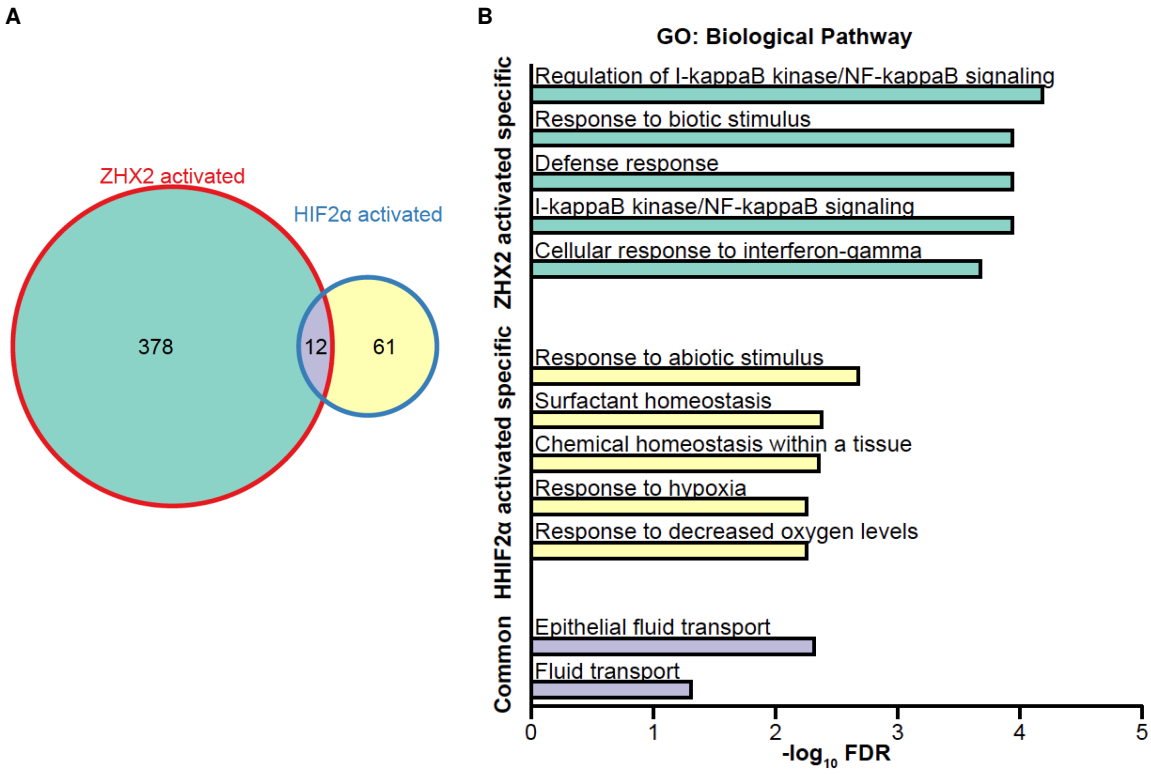


**Figure S11. ZHX2 and HIF2α regulates distinctive pathways in ccRCC.**
**(A)** Venn diagram Analysis of ZHX2 and HIF2α positively regulated genes. HIF2α activated target genes in 786-O were analyzed from HIF2α siRNA RNA-seq data available online (GSE102097) *(23)*.
**(B)** Gene Ontology (GO) analysis of ZHX2 and HIF2α positively regulated target genes.

## Figure S12

**A**

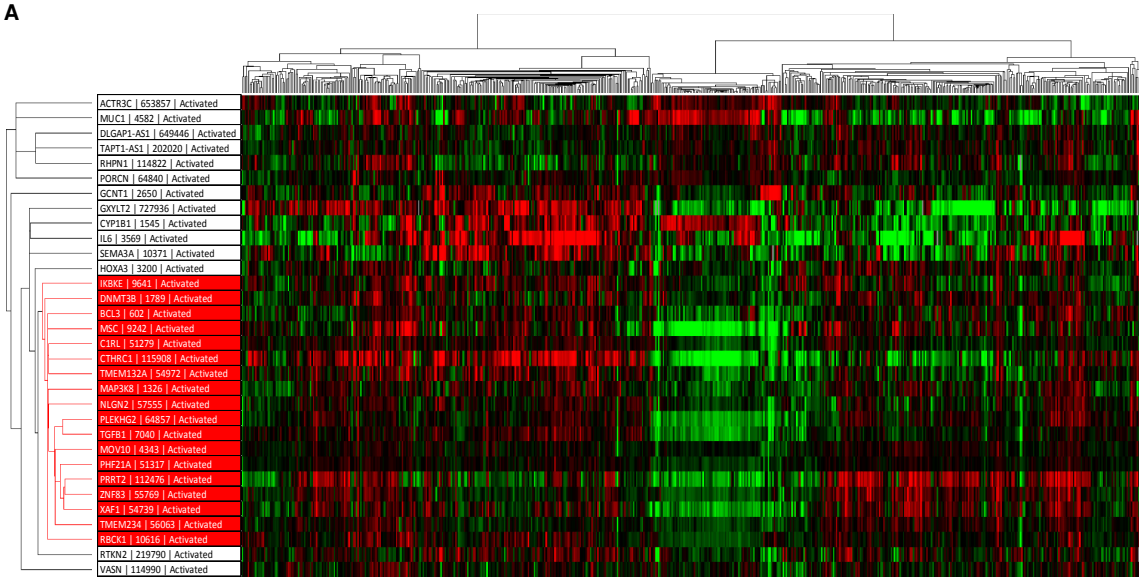


**B**

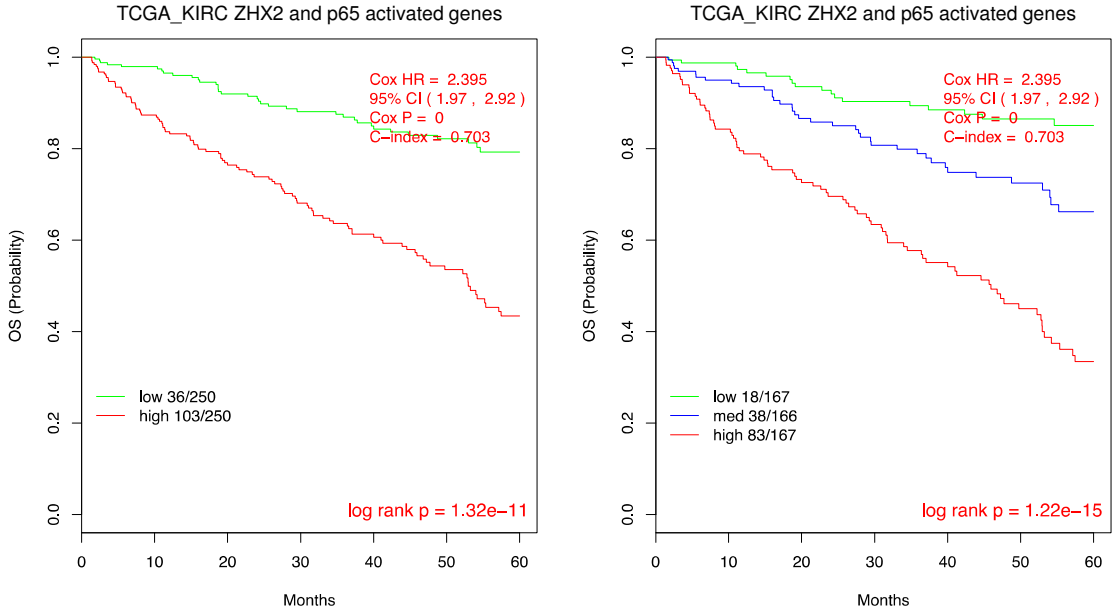

**Figure S12. ZHX2 and p65 activated genes predict worse prognosis in kidney cancer.** **(A)** Heatmap of gene expression of 32 genes that correlates with prognosis and first identified in our microarray data set, and now further analyzed using the kidney cancers from TCGA dataset. The highlighted red region indicates 18 genes that showed an expression correlation above 0.5, thus showing moderate to high correlation across a large and diverse set of kidney cancers.
**(B)** Survival analysis for overall survival (OS) of kidney cancer patients using the median expression values of the 18 genes identified by cluster analysis from S12A. Note that these genes are a subset of the ZHX2 and p65 activated genes, whose higher expression associates with poorer survival. On the left panel, patients were divided into two groups based upon the patients rank order median expression of these 18 genes, and on the right panel, patients were stratified into three groups based upon low, medium and high expression values.

**Figure S13**

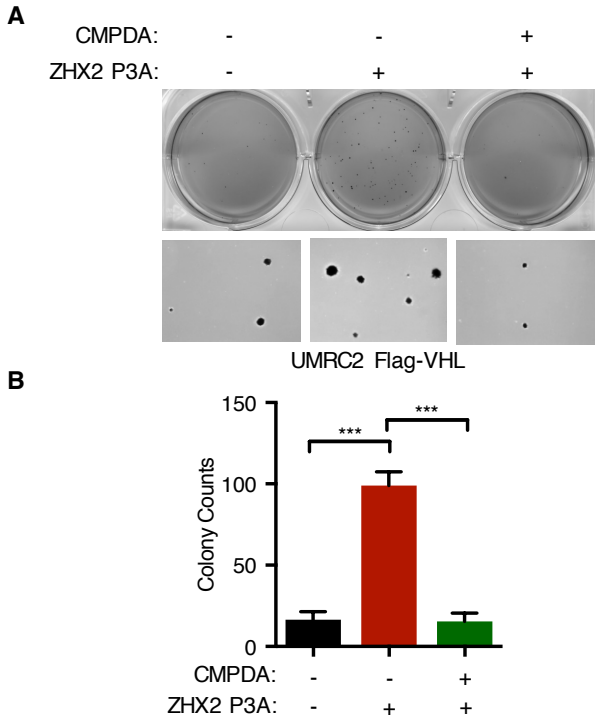


**Figure S13. ZHX2P3A promotes soft agar growth in NF-κB dependent manner.**
**(A-B)** Soft agar growth (A) and its quantification (B) of UMRC2 cells which infected with lentivirus encoding Flag-VHL followed by transfection with HA-ZHX2 P3A with or without CMPDA (5 μM) daily treatment.
Error bars represent mean ± SEM, n=3 replicates per group, unpaired *t*-test. *** denotes p value of <0.005.

**Figure S14**

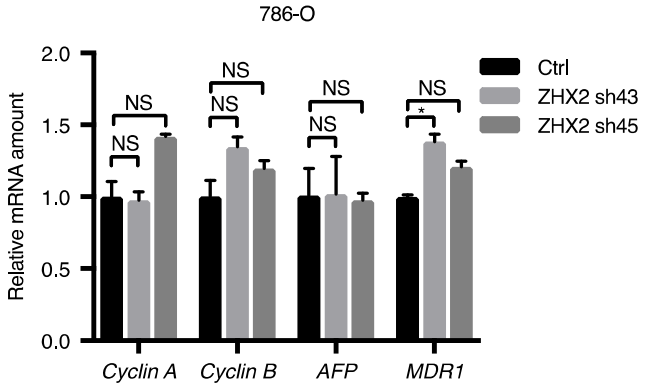


**Figure S14. ZHX2 depletion has no effect on Cyclin A, Cyclin B, AFP and MDR1 expression in ccRCC.**

Relative mRNA amount from ZHX2 shRNA microarray analysis in 786-O. Error bars represent mean ± SEM, unpaired *t*-test. * denotes p value of <0.05. NS denotes "non-significant".

**Table S1. VHL mutation status from ccRCC patient tissues**

| Sample | GeneName | Effect2 | Chr | Position | Ref | Alt | Mutation |
|---|---|---|---|---|---|---|---|
| 141_T | VHL | SPLICE_SITE_ACCEPTOR | chr3 | 10191470 | G | T | N/A |
| 169_T | VHL | NON_SYNONYMOUS_CODING | chr3 | 10191492 | G | A | p.Cys162Tyr |
| 332_T | VHL | NON_SYNONYMOUS_CODING | chr3 | 10183725 | C | T | p.Ser65Leu |
| 452_T | VHL | FRAME_SHIFT | chr3 | 10183740 | AG | A | c.209*>-G |
| 703_T | VHL | NON_SYNONYMOUS_CODING | chr3 | 10183788 | C | T | p.Pro86Leu |
| 778_T | VHL | NON_SYNONYMOUS_CODING | chr3 | 10183771 | T | A | p.Ser80Arg |
| 936_T | VHL | NON_SYNONYMOUS_CODING | chr3 | 10191501 | T | A | p.Val165Asp |
| | | | | | | | |
| 860_T | VHL | FRAME_SHIFT | chr3 | 10191504 | TC | T | c.374*>-C |
| 498_T | VHL | FRAME_SHIFT | chr3 | 10183756 | CTTCTGCA | C | c.225*>-TTCTGCA |

**Table S2. Quantification of IHC staining for ZHX2 (listed online separately)**

**Table S3. ZHX2 and HIF2α positively regulated gene list**

| Targets of ZHX2 only | Common targets | Targets of HIF2α only |
|---|---|---|
| UBB, SLC25A3, MUC22, RASA4B, LINC00476, PCMTD2, SCD, TLN2, ITGAV, JAK1, LOXL2, ECI1, CSF1, IRF9, SLC25A1, TTYH3, RBCK1, AKR1B1, RNF213, ABCA1, ITSN1, FNBP1L, KCTD3, PBX2, COL7A1, SQLE, ZBTB38, RMRP, MAN2C1, SEC14L6, NLGN2, KIAA1217, TMEM2, MSMO1, DDB2, TGFB1, MLLT1, SREBF2, EGFR, SH3BP2, GAS2L3, IRX5, TMEM47, RUNX1-IT1, BBS2, SLC2A4RG, LYRM1, PLEKHG2, POLM, EOGT, PHKA2, PHF21A, TMEM65, NPDC1, ZNF618, STEAP3, FAT1, STARD4, SAMD9, ZMIZ2, XAF1, HGD, PITX2, CELSR1, STAT6, SLC6A6, C1QTNF6, PDZK1IP1, SLC44A2, MVP, MOV10, DDX60, SHISA4, SNX10, TMEM234, AHNAK2, IQSEC2, PORCN, MAN1A1, TNFSF10, PGBD5, TRIM38, FAM117B, HGSNAT, KRCC1, CDHR1, EEPD1, ALDH3B1,HOOK2, MID1, KLF12, ZFYVE1, SLC22A18, TNIP1, RBPMS, NMRK1, CACNB3, MIR151B, NRBP2, ENOSF1, SERPINF2, ADAMTS9, TP53, TNS3, PTPRM, FZD2, DNM2, NALCN-AS1, TMEM132A, NEDD9, GABBR1, CAPN12, INSIG1, MEGF6, ZNF83, SCN9A, MIR4525, BAMBI, C1orf106, PTGER2, CTHRC1, ZDHHC1, EPHB2, IFI44, ABLIM1, TAS2R4, TRIM5, MRAS, CACHD1, TCIRG1, MGLL, HOXA3, RNF212, IKBKE, TNS1, SYNGAP1, TSC22D3, C5orf56, MMAA, D2HGDH, GXYLT2, ARSA, ABCA2, DSE, SLC6A12, LXN, ARHGEF6, GCNT1, OPTN, NUP62CL, DLGAP1-AS1, JUNB, ITIH2, PHKA2-AS1, CYP2E1, FAM20C, ADD3, DDX60L, BRINP1, LSS, RYR3, MUC1, CYP4V2, HMGCS1, TTLL1, PAX6, MFNG, LOC100128494, LOC653160, CAPS2, IL6, KLHDC1, TSPAN12, FGFR3, LOC494127, SHROOM4, FAM122C, ABCC2, CARD6, HOXA-AS2, HLX, KY, GRB7, NID2, ARHGAP29, DNAH1, BCORP1, HECW1, RASSF4, IFI35, NXNL2, BCL3, MAF, FAM149A, ARSD, TBC1D8, OLFML2A, TAPT1-AS1, TLL1, TMEM91, MAML2, PER1, MSC, PLD1, DMRTA1, HOOK1, DNMT3B, TM4SF18, SORCS2, C1RL, FMO4, GDPD3, RTKN2, H6PD, MIR604, PLXND1, HCFC1R1, SVIL, EGR2, MIR4803, DDX58, HECW2, LOC553103, TLR3, PPP4R4, PER3, PTPRD, MIR181B2, SLC6A13, SGK2, UNC13C, PDGFB, SLC4A4, ZNF117, LIPG, PTGES, PCDHGB8P, RHPN1, DLGAP1-AS3, CCDC146, SFRP4, ATP1B1, MITF, ARSD-AS1, ABCC6, MAMDC4, IFIH1, PLEKHH2, MCTP1, P2RX4, UBA7, MTMR11, KBTBD3, NEFL, S1PR1, TNFAIP3, FOXP2, ARSE, ANKS1B, ESX1, BCL2L11, EPB41L4A, GLCCI1, SMR3A, WDR78, B3GNT4, GUCA1C, TRIM22, CNR1, JAM2, ADAMTS9-AS2, F8, FHDC1, HSD17B7P2, ACTR3C, SLN, HNF1A-AS1, DAPK1, SLC16A4, PRRT2, OAS2, MMP1, FBXL13, SLC44A3, EGR1, VASN, SIPA1L2, PLCB1, PRKCQ, MAP7D2, GBP2, MTSS1, SAMD9L, DSCAML1, QPRT, KANSL1L, RASSF9, FGFR4, OLFML2B, DCLK1, VSTM4, LOC441204, RNF144B, ZHX2, FRMD4B, PTPN13, IL1R1, MIR3974, DHRS9, BCL2, CD24, NPY1R, STAT1, SEMA3A, PELI1, HNF1B, SEMA6D, SPINK13, FRK, CST1, DGCR9, FCAMR, MS4A3, ARL14EPL, CA2, CDKL5, DNAJB13, ASTN2, SORBS1, C10orf62, CKAP5, MIR3936, C1orf186, LOC100506895, CYP1B1, SGPP2, GMNC, LINC00410, OAS1, LOC440300, GABRG1, CTSO, EFHB, SAA1, PLEK, C14orf105, LHFPL3-AS2, SMPDL3A, GPRIN3, IMPA2, GPRC5B, SLC2A2, MIR1302-7, LRRC37A3, ACMSD, VCAM1, CCL2, ATP8A1, VAV3, MAB21L3, CLEC4E, MIR516B2, CXCL8, C3, KIF12, SLC17A1, TINAG, ITGB6, IFI44L, ENPP3, ABCA12. | ARRDC3, CP, EDN1, ITPR1, LUCAT1, MAP3K8, PSORS1C3, RNASET2, SEMA6A, SYNPO, TMEM141, TNFAIP6 | ACKR3, ADM, APOL1, APOL2, BHLHE40, C10orf10, C1QL1, C5orf46, CA12, CCND1, DDIT4, EGLN3, EPAS1, ERRFI1, F3, FZD8, GAL3ST1, HIST1H1T, IGFL1, INHBB, IRS2, ITGB8, KLF13, KMO, LINC00704, LINC01320, LOC100506498, LOC613266, LPCAT1, LSM5, MACROD2, MIR155HG, MIR193BHG, MOB3A, MYEOV, NDRG1, NECAB1, PLEKHG4B, PLIN2, PPP1R14C, PPP1R3B, RAB42, RIPK4, RNA28S4, RNA28S5, RNA45S4, RNA45S5, SAPCD2, SEMA4B, SLC2A1, SLCO4A1, SMIM3, SPNS2, STC1, TGFA, TGM2, TMEM64, TRIB3, UBALD2, VEGFA, ZNF395 |

**Table S4. Microarray data (LogFC value) for 390 genes positively regulated by both ZHX2 and RelA/p65 in ccRCC**

| Gene | ZHX2_scr1 | ZHX2_scr2 | ZHX2_sh45_1 | ZHX2_sh45_2 | p65_scr1 | p65_scr2 | p65_sh1 | p65_sh2 |
|---|---|---|---|---|---|---|---|---|
| UBB | 9.805 | 9.7 | 9.73 | 9.76 | 8.93 | 8.95 | 8.94 | 8.86 |
| SLC25A3 | 7.67 | 7.76 | 7.69 | 7.72 | 4.37 | 4.96 | 3.99 | 2.05 |
| MUC22 | 7.79 | 7.73 | 7.72 | 7.615 | 3.29 | 2.79 | 2.86 | 3.01 |
| RASA4B | 7.65 | 7.61 | 7.45 | 7.42 | 3.45 | 3.73 | 3.49 | 2.81 |
| LINC00476 | 6.37 | 6.04 | 5.94 | 6.12 | 2.35 | 2.10 | 1.84 | 2.13 |
| PCMTD2 | 8.025 | 7.945 | 7.81 | 7.695 | 5.39 | 5.30 | 5.09 | 5.11 |
| SCD | 12.45 | 12.39 | 12 | 11.94 | 11.03 | 11.03 | 9.85 | 9.99 |
| TLN2 | 7.74 | 7.69 | 7.4 | 7.43 | 5.89 | 5.51 | 5.55 | 5.25 |
| ITGAV | 11.59 | 11.58 | 11.09 | 11.15 | 10.16 | 9.58 | 9.91 | 9.80 |
| JAK1 | 11.62 | 11.53 | 11.1 | 11.09 | 10.25 | 10.16 | 9.85 | 10.01 |
| LOXL2 | 11.98 | 12.01 | 11.46 | 11.53 | 9.07 | 8.94 | 8.62 | 8.81 |
| ECI1 | 10.13 | 10.07 | 9.67 | 9.68 | 7.02 | 7.04 | 7.07 | 6.94 |
| CSF1 | 10.29 | 10.27 | 9.81 | 9.88 | 7.42 | 7.14 | 7.16 | 7.06 |
| IRF9 | 8.015 | 8.04 | 7.645 | 7.73 | 3.73 | 3.63 | 2.94 | 3.43 |
| SLC25A1 | 11.11 | 11.02 | 10.6 | 10.59 | 7.85 | 7.75 | 7.54 | 7.52 |
| TTYH3 | 10.58 | 10.54 | 10.07 | 10.15 | 9.28 | 9.28 | 8.91 | 8.79 |
| RBCK1 | 10.72 | 10.84 | 10.35 | 10.29 | 7.68 | 7.81 | 7.78 | 7.50 |
| AKR1B1 | 11.5 | 11.45 | 10.99 | 10.98 | 6.93 | 6.82 | 6.39 | 6.22 |
| RNF213 | 10.94 | 10.83 | 10.39 | 10.44 | 8.05 | 7.98 | 7.31 | 7.47 |
| ABCA1 | 10.89 | 10.82 | 10.37 | 10.4 | 9.33 | 8.47 | 8.34 | 8.39 |
| ITSN1 | 9.74 | 9.67 | 9.32 | 9.24 | 6.49 | 6.07 | 5.61 | 5.81 |
| FNBP1L | 9.79 | 9.73 | 9.33 | 9.31 | 8.07 | 8.07 | 7.67 | 7.76 |
| ARRDC3 | 11.44 | 11.35 | 10.85 | 10.89 | 8.80 | 9.19 | 8.45 | 8.44 |
| KCTD3 | 10.54 | 10.45 | 9.99 | 10.03 | 7.81 | 7.63 | 7.45 | 7.51 |
| PBX2 | 8.36 | 8.265 | 7.92 | 7.935 | 5.42 | 4.99 | 4.30 | 4.62 |
| COL7A1 | 9.08 | 9.15 | 8.71 | 8.67 | 4.56 | 4.45 | 4.39 | 4.26 |
| SQLE | 9.82 | 9.85 | 9.37 | 9.38 | 8.44 | 8.44 | 7.92 | 7.56 |
| ZBTB38 | 10.47 | 10.44 | 9.89 | 10.03 | 5.96 | 6.07 | 5.89 | 6.14 |
| RMRP | 12.09 | 11.92 | 11.47 | 11.39 | 11.65 | 11.58 | 11.58 | 11.50 |
| MAN2C1 | 9.17 | 9.15 | 8.69 | 8.75 | 4.18 | 3.84 | 3.76 | 4.02 |
| SEC14L6 | 9.08 | 9.17 | 8.73 | 8.64 | 6.11 | 6.49 | 6.12 | 6.28 |
| NLGN2 | 9.005 | 8.9 | 8.55 | 8.49 | 5.24 | 4.98 | 5.07 | 4.98 |
| KIAA1217 | 9.89 | 9.96 | 9.47 | 9.42 | 6.22 | 6.33 | 5.95 | 6.12 |
| TMEM2 | 9.31 | 9.26 | 8.8 | 8.86 | 7.89 | 7.18 | 7.23 | 7.32 |
| MSMO1 | 10.71 | 10.71 | 10.08 | 10.29 | 9.77 | 9.74 | 8.87 | 8.55 |
| DDB2 | 10.45 | 10.29 | 9.91 | 9.81 | 6.61 | 6.96 | 6.24 | 6.23 |
| TGFB1 | 10.9 | 10.77 | 10.34 | 10.26 | 9.05 | 8.63 | 8.54 | 8.40 |
| LUCAT1 | 9.59 | 9.46 | 9.01 | 9.09 | 4.32 | 5.33 | 3.85 | 3.32 |
| MLLT1 | 10.05 | 10 | 9.59 | 9.46 | 7.82 | 7.98 | 7.75 | 7.74 |
| SREBF2 | 9.48 | 9.5 | 9.01 | 9.01 | 7.26 | 7.28 | 6.74 | 6.63 |
| SYNPO | 10.63 | 10.65 | 10.08 | 10.12 | 7.46 | 7.76 | 6.69 | 6.65 |
| EGFR | 11.24 | 11.14 | 10.59 | 10.65 | 9.22 | 8.83 | 8.15 | 8.42 |
| SH3BP2 | 8.25 | 8.21 | 7.82 | 7.8 | 4.86 | 4.52 | 4.52 | 4.70 |
| GAS2L3 | 9.98 | 9.99 | 9.44 | 9.49 | 7.86 | 8.14 | 7.75 | 7.73 |
| IRX5 | 8.62 | 8.7 | 8.24 | 8.17 | 4.82 | 4.32 | 4.24 | 3.79 |
| TMEM47 | 10.51 | 10.47 | 9.94 | 9.93 | 8.28 | 7.76 | 7.35 | 7.53 |
| RUNX1-IT1 | 9.31 | 9.24 | 8.84 | 8.71 | 3.16 | 3.37 | 2.18 | 2.48 |
| BBS2 | 9.13 | 9.03 | 8.57 | 8.61 | 6.39 | 6.15 | 6.03 | 6.11 |
| SLC2A4RG | 10.58 | 10.54 | 9.99 | 9.98 | 7.71 | 7.45 | 6.77 | 6.68 |

| | | | | | | | | |
|---|---|---|---|---|---|---|---|---|
| LYRM1 | 9.33 | 9.13 | 8.73 | 8.71 | 7.26 | 7.44 | 6.62 | 6.73 |
| PLEKHG2 | 8.55 | 8.47 | 8.08 | 7.98 | 4.84 | 4.45 | 4.74 | 4.39 |
| POLM | 7.86 | 7.83 | 7.42 | 7.38 | 3.79 | 3.40 | 3.24 | 3.57 |
| EOGT | 9.82 | 9.73 | 9.26 | 9.18 | 7.82 | 7.83 | 7.77 | 7.86 |
| PHKA2 | 10.11 | 10.13 | 9.54 | 9.55 | 6.01 | 6.12 | 5.41 | 5.33 |
| RNASET2 | 10.56 | 10.54 | 9.96 | 9.93 | 4.83 | 4.82 | 4.15 | 4.60 |
| PHF21A | 9.32 | 9.13 | 8.72 | 8.67 | 6.79 | 6.74 | 6.08 | 6.32 |
| TMEM65 | 9.77 | 9.59 | 9.14 | 9.1 | 7.62 | 8.13 | 7.59 | 7.58 |
| NPDC1 | 8.36 | 8.39 | 7.88 | 7.9 | 5.55 | 5.45 | 5.64 | 5.33 |
| ZNF618 | 9.19 | 9.03 | 8.55 | 8.61 | 6.85 | 6.90 | 6.82 | 6.69 |
| STEAP3 | 10.76 | 10.67 | 10.09 | 10.08 | 7.53 | 7.14 | 7.20 | 7.16 |
| FAT1 | 9.31 | 9.21 | 8.72 | 8.71 | 7.33 | 6.96 | 6.44 | 6.31 |
| STARD4 | 8.58 | 8.45 | 8.04 | 7.98 | 6.66 | 7.31 | 6.28 | 6.32 |
| SAMD9 | 9.12 | 9.03 | 8.55 | 8.52 | 6.83 | 6.69 | 6.68 | 6.70 |
| ZMIZ2 | 9.76 | 9.78 | 9.13 | 9.24 | 6.19 | 6.17 | 6.04 | 5.84 |
| XAF1 | 9.4 | 9.45 | 8.8 | 8.92 | 5.48 | 5.54 | 5.39 | 5.01 |
| HGD | 8.85 | 8.97 | 8.39 | 8.36 | 5.78 | 5.37 | 5.09 | 4.55 |
| PITX2 | 7.77 | 7.86 | 7.37 | 7.32 | 4.04 | 4.51 | 4.03 | 4.25 |
| CELSR1 | 9.38 | 9.22 | 8.75 | 8.73 | 6.87 | 6.12 | 5.98 | 6.26 |
| STAT6 | 9.46 | 9.45 | 8.93 | 8.84 | 8.11 | 7.86 | 7.65 | 7.47 |
| SLC6A6 | 10.43 | 10.29 | 9.74 | 9.73 | 8.28 | 8.48 | 7.02 | 7.64 |
| C1QTNF6 | 9.01 | 8.87 | 8.43 | 8.37 | 4.31 | 4.53 | 4.25 | 4.44 |
| PDZK1IP1 | 9.47 | 9.45 | 8.84 | 8.93 | 8.04 | 7.61 | 6.94 | 7.34 |
| SLC44A2 | 10.12 | 9.95 | 9.4 | 9.45 | 7.94 | 7.69 | 6.15 | 6.54 |
| MVP | 9.48 | 9.47 | 8.99 | 8.8 | 7.98 | 7.88 | 7.60 | 7.73 |
| MOV10 | 10.77 | 10.62 | 10.02 | 10.06 | 7.61 | 7.40 | 7.09 | 7.16 |
| DDX60 | 9.31 | 9.06 | 8.65 | 8.59 | 5.73 | 5.45 | 5.42 | 5.41 |
| SHISA4 | 8.59 | 8.54 | 8.12 | 7.95 | 5.24 | 5.26 | 5.12 | 4.72 |
| SNX10 | 7.12 | 7.1 | 6.66 | 6.68 | 4.66 | 4.09 | 4.43 | 4.06 |
| TMEM234 | 8.56 | 8.55 | 8.04 | 8.01 | 3.82 | 4.25 | 4.09 | 3.68 |
| AHNAK2 | 8.73 | 8.54 | 8.08 | 8.12 | 6.33 | 5.87 | 5.87 | 6.15 |
| IQSEC2 | 7.84 | 7.81 | 7.34 | 7.34 | 4.43 | 4.29 | 4.36 | 4.34 |
| PORCN | 10.58 | 10.47 | 9.85 | 9.88 | 7.55 | 8.40 | 7.63 | 7.67 |
| MAN1A1 | 9.2 | 9.19 | 8.67 | 8.56 | 6.66 | 6.14 | 6.27 | 6.07 |
| TNFSF10 | 12.45 | 12.42 | 11.67 | 11.63 | 10.81 | 11.01 | 10.00 | 10.20 |
| PGBD5 | 7.42 | 7.46 | 6.98 | 6.96 | 4.25 | 3.82 | 2.55 | 2.22 |
| TRIM38 | 9.59 | 9.54 | 8.96 | 8.96 | 7.57 | 6.96 | 7.20 | 7.29 |
| FAM117B | 9.85 | 9.84 | 9.23 | 9.21 | 8.51 | 8.57 | 8.38 | 8.30 |
| HGSNAT | 9.18 | 9.05 | 8.56 | 8.51 | 7.70 | 7.40 | 7.43 | 7.39 |
| KRCC1 | 9.58 | 9.57 | 8.96 | 8.97 | 7.77 | 7.69 | 7.83 | 7.53 |
| CDHR1 | 7.07 | 7.06 | 6.58 | 6.64 | 2.80 | 2.79 | 2.53 | 2.87 |
| EEPD1 | 7.74 | 7.73 | 7.23 | 7.24 | 4.92 | 4.62 | 4.94 | 4.45 |
| ALDH3B1 | 9.8 | 9.82 | 9.24 | 9.11 | 6.50 | 6.06 | 4.64 | 5.00 |
| HOOK2 | 8.72 | 8.73 | 8.1 | 8.22 | 4.06 | 4.75 | 4.44 | 4.18 |
| MID1 | 9.88 | 9.86 | 9.18 | 9.28 | 6.78 | 6.62 | 6.54 | 6.66 |
| KLF12 | 9.37 | 9.23 | 8.72 | 8.67 | 6.19 | 6.34 | 6.25 | 6.11 |
| ZFYVE1 | 7.61 | 7.67 | 7.12 | 7.15 | 5.16 | 5.05 | 4.80 | 4.71 |
| SLC22A18 | 8.51 | 8.39 | 7.83 | 7.95 | 5.03 | 3.78 | 3.07 | 3.90 |
| TNIP1 | 9.54 | 9.75 | 9.02 | 8.98 | 7.61 | 7.53 | 7.04 | 6.97 |
| RBPMS | 9.31 | 9.22 | 8.61 | 8.68 | 6.21 | 5.85 | 5.28 | 5.24 |
| NMRK1 | 7.49 | 7.4 | 6.91 | 6.98 | 4.68 | 4.45 | 4.17 | 4.00 |
| CACNB3 | 8.69 | 8.82 | 8.16 | 8.17 | 5.27 | 5.08 | 5.14 | 4.88 |
| MIR151B | 8.49 | 8.56 | 8.04 | 7.86 | 3.31 | 3.51 | 3.35 | 3.37 |
| NRBP2 | 9.15 | 9.23 | 8.52 | 8.62 | 4.91 | 5.26 | 5.06 | 5.00 |
| ENOSF1 | 8.9 | 8.99 | 8.38 | 8.3 | 6.03 | 5.89 | 5.05 | 5.20 |
| SERPINF2 | 7.08 | 7.01 | 6.49 | 6.64 | 3.09 | 2.22 | 2.39 | 2.17 |

| | | | | | | | | |
|---|---|---|---|---|---|---|---|---|
| ADAMTS9 | 10.29 | 10.22 | 9.53 | 9.58 | 7.21 | 7.05 | 6.71 | 6.52 |
| TP53 | 9.16 | 8.99 | 8.47 | 8.44 | 7.39 | 7.52 | 6.60 | 6.93 |
| TNS3 | 9.5 | 9.36 | 8.82 | 8.75 | 6.78 | 6.19 | 5.92 | 5.91 |
| PTPRM | 11.15 | 11.02 | 10.31 | 10.34 | 7.55 | 7.17 | 7.33 | 7.27 |
| FZD2 | 7.46 | 7.32 | 6.81 | 6.95 | 5.00 | 3.91 | 3.94 | 3.77 |
| DNM2 | 10.24 | 10.17 | 9.51 | 9.49 | 6.19 | 5.73 | 5.85 | 5.95 |
| NALCN-AS1 | 6.68 | 6.58 | 6.15 | 6.19 | 2.45 | 2.43 | 2.21 | 2.52 |
| TMEM132A | 8.55 | 8.57 | 7.96 | 7.97 | 4.79 | 4.31 | 4.58 | 3.65 |
| NEDD9 | 7.5 | 7.44 | 6.98 | 6.92 | 3.28 | 3.87 | 3.35 | 2.62 |
| GABBR1 | 9.72 | 9.8 | 9.05 | 9.1 | 4.21 | 4.20 | 3.95 | 3.81 |
| CAPN12 | 7.36 | 7.44 | 6.87 | 6.89 | 2.20 | 2.23 | 2.39 | 1.77 |
| INSIG1 | 11.34 | 11.4 | 10.58 | 10.56 | 10.00 | 9.86 | 9.39 | 9.12 |
| MEGF6 | 7.63 | 7.56 | 7.1 | 7.02 | 1.83 | 2.71 | 1.64 | 1.72 |
| ZNF83 | 10.01 | 9.82 | 9.16 | 9.27 | 4.24 | 4.01 | 3.90 | 4.08 |
| SCN9A | 8.66 | 8.62 | 8.05 | 8.01 | 5.00 | 4.82 | 4.49 | 5.22 |
| MIR4525 | 10.77 | 11.11 | 10.14 | 10.19 | 5.68 | 5.01 | 4.92 | 4.53 |
| BAMBI | 8.8 | 8.68 | 8.17 | 8.06 | 7.80 | 7.04 | 7.28 | 7.41 |
| C1orf106 | 8.45 | 8.47 | 7.8 | 7.91 | 4.80 | 5.07 | 4.75 | 4.85 |
| PTGER2 | 7.69 | 7.81 | 7.12 | 7.27 | 4.03 | 4.35 | 3.46 | 3.00 |
| PSORS1C3 | 8.135 | 8.15 | 7.47 | 7.625 | 1.59 | 1.64 | 1.23 | 1.48 |
| TMEM141 | 9.73 | 9.63 | 8.94 | 8.99 | 6.25 | 6.59 | 5.67 | 5.95 |
| CTHRC1 | 7.66 | 7.58 | 6.95 | 7.16 | 5.55 | 5.28 | 4.35 | 4.67 |
| ZDHHC1 | 8.29 | 8.24 | 7.66 | 7.64 | 4.97 | 4.95 | 4.50 | 4.94 |
| EPHB2 | 9.25 | 9.07 | 8.61 | 8.34 | 6.73 | 6.50 | 6.13 | 6.14 |
| IFI44 | 9.19 | 9.07 | 8.43 | 8.46 | 4.48 | 3.52 | 3.74 | 3.59 |
| ABLIM1 | 9.41 | 9.51 | 8.7 | 8.8 | 8.08 | 7.93 | 7.92 | 7.85 |
| TAS2R4 | 8.5 | 8.39 | 7.76 | 7.86 | 2.11 | 2.40 | 2.10 | 2.11 |
| TRIM5 | 8.26 | 8.05 | 7.53 | 7.55 | 3.71 | 3.70 | 3.27 | 3.86 |
| MRAS | 8.35 | 8.32 | 7.73 | 7.68 | 5.65 | 5.76 | 4.95 | 4.71 |
| CACHD1 | 9.1 | 8.88 | 8.41 | 8.21 | 7.49 | 6.47 | 6.57 | 6.18 |
| TCIRG1 | 9.78 | 9.7 | 9.05 | 8.94 | 5.65 | 5.21 | 4.91 | 5.06 |
| MGLL | 9.35 | 9.3 | 8.66 | 8.56 | 5.75 | 5.48 | 5.14 | 5.13 |
| HOXA3 | 8.47 | 8.47 | 7.91 | 7.73 | 6.45 | 6.43 | 6.44 | 6.42 |
| RNF212 | 6.71 | 6.82 | 6.2 | 6.29 | 2.58 | 2.03 | 1.90 | 1.77 |
| IKBKE | 8.4 | 8.34 | 7.74 | 7.71 | 5.42 | 5.35 | 4.34 | 4.46 |
| TNS1 | 8.79 | 8.82 | 8.16 | 8.09 | 4.46 | 4.18 | 3.70 | 3.89 |
| SYNGAP1 | 8.345 | 8.205 | 7.725 | 7.54 | 3.83 | 4.29 | 4.12 | 3.97 |
| TSC22D3 | 7.85 | 7.99 | 7.28 | 7.33 | 3.06 | 3.54 | 2.95 | 2.72 |
| C5orf56 | 8.38 | 8.34 | 7.84 | 7.58 | 3.11 | 3.10 | 3.14 | 3.03 |
| MMAA | 7.34 | 7.45 | 6.76 | 6.88 | 5.74 | 5.54 | 5.49 | 5.59 |
| D2HGDH | 7.94 | 7.74 | 7.33 | 7.13 | 2.76 | 2.89 | 2.82 | 2.52 |
| GXYLT2 | 10.67 | 10.66 | 9.84 | 9.82 | 8.09 | 8.08 | 7.03 | 7.17 |
| ARSA | 8.58 | 8.65 | 7.93 | 7.95 | 4.48 | 4.46 | 4.01 | 4.31 |
| ABCA2 | 10.26 | 10.14 | 9.37 | 9.43 | 6.09 | 6.04 | 5.94 | 5.66 |
| DSE | 6.91 | 6.95 | 6.42 | 6.35 | 4.33 | 3.61 | 3.44 | 3.23 |
| SLC6A12 | 7.52 | 7.61 | 7 | 6.94 | 3.20 | 2.85 | 2.30 | 1.92 |
| LXN | 8.38 | 8.2 | 7.65 | 7.62 | 5.29 | 5.10 | 4.43 | 5.12 |
| ARHGEF6 | 9.01 | 8.96 | 8.31 | 8.24 | 6.47 | 7.22 | 6.10 | 6.25 |
| GCNT1 | 10.32 | 10.16 | 9.41 | 9.45 | 7.31 | 7.20 | 6.74 | 6.82 |
| OPTN | 9.02 | 8.92 | 8.31 | 8.21 | 7.48 | 7.28 | 7.08 | 7.17 |
| NUP62CL | 7.32 | 7.33 | 6.72 | 6.77 | 1.91 | 2.91 | 1.76 | 1.73 |
| DLGAP1-AS1 | 8.27 | 7.98 | 7.47 | 7.49 | 4.79 | 5.36 | 4.98 | 4.95 |
| JUNB | 10.07 | 9.94 | 9.16 | 9.26 | 8.28 | 7.75 | 7.70 | 7.78 |
| ITIH2 | 6.25 | 6.17 | 5.8 | 5.63 | 2.02 | 2.08 | 1.89 | 1.88 |
| PHKA2-AS1 | 6.44 | 6.66 | 6.02 | 6.03 | 1.74 | 1.36 | 1.01 | 1.62 |
| CYP2E1 | 6.75 | 6.83 | 6.17 | 6.32 | 1.75 | 2.08 | 1.46 | 2.19 |

| | | | | | | | | |
|---|---|---|---|---|---|---|---|---|
| FAM20C | 8.68 | 8.76 | 8.06 | 7.98 | 5.20 | 5.50 | 5.26 | 5.04 |
| ADD3 | 8.61 | 8.57 | 7.87 | 7.93 | 6.11 | 5.49 | 4.83 | 4.91 |
| DDX60L | 9.1 | 8.94 | 8.33 | 8.26 | 5.80 | 5.34 | 5.00 | 5.00 |
| BRINP1 | 8.85 | 8.55 | 7.94 | 8.05 | 5.96 | 5.71 | 4.97 | 4.86 |
| LSS | 9.28 | 9.21 | 8.51 | 8.48 | 7.45 | 7.30 | 5.49 | 5.84 |
| RYR3 | 6.01 | 6.07 | 5.52 | 5.58 | 1.07 | 1.24 | 1.00 | 0.98 |
| MUC1 | 7.43 | 7.34 | 6.82 | 6.75 | 3.55 | 4.70 | 3.28 | 3.61 |
| CYP4V2 | 8.19 | 8.01 | 7.49 | 7.39 | 3.68 | 4.49 | 3.48 | 3.19 |
| HMGCS1 | 8.73 | 8.69 | 8.02 | 7.98 | 8.40 | 7.95 | 6.83 | 6.88 |
| TTLL1 | 8.17 | 7.9 | 7.36 | 7.4 | 4.89 | 4.16 | 4.16 | 3.88 |
| PAX6 | 6.45 | 6.49 | 5.92 | 5.96 | 3.22 | 2.81 | 3.03 | 2.42 |
| MFNG | 8.97 | 8.57 | 8.05 | 8.05 | 2.90 | 3.99 | 3.34 | 3.35 |
| LOC100128494 | 7.23 | 7.25 | 6.62 | 6.67 | 3.79 | 3.38 | 3.34 | 3.70 |
| LOC653160 | 8.25 | 8.11 | 7.54 | 7.47 | 3.77 | 4.12 | 3.29 | 3.32 |
| CAPS2 | 6.36 | 6.35 | 5.9 | 5.76 | 2.35 | 1.58 | 1.50 | 1.18 |
| IL6 | 7.68 | 7.92 | 7.08 | 7.23 | 4.31 | 5.03 | 3.12 | 3.12 |
| KLHDC1 | 6.71 | 6.83 | 6.27 | 6.15 | 1.67 | 2.40 | 1.35 | 1.66 |
| TSPAN12 | 8.04 | 8.03 | 7.34 | 7.4 | 5.19 | 4.25 | 4.36 | 4.39 |
| FGFR3 | 7.03 | 7.19 | 6.58 | 6.46 | 2.10 | 2.60 | 2.19 | 2.25 |
| LOC494127 | 5.72 | 5.89 | 5.34 | 5.3 | 1.90 | 1.20 | 1.63 | 1.15 |
| SHROOM4 | 8.31 | 8.04 | 7.5 | 7.48 | 4.36 | 3.84 | 3.41 | 3.89 |
| FAM122C | 8.25 | 8.08 | 7.46 | 7.5 | 3.52 | 3.11 | 3.16 | 3.26 |
| ABCC2 | 7.46 | 7.19 | 6.68 | 6.74 | 4.33 | 2.79 | 2.62 | 2.37 |
| CARD6 | 6.8 | 6.82 | 6.28 | 6.19 | 5.83 | 5.48 | 5.02 | 5.32 |
| HOXA-AS2 | 8.16 | 7.98 | 7.44 | 7.33 | 5.54 | 5.37 | 5.16 | 5.24 |
| HLX | 7.83 | 8.04 | 7.27 | 7.25 | 4.69 | 4.09 | 4.01 | 4.12 |
| KY | 7.69 | 7.77 | 7.11 | 7.02 | 3.59 | 3.56 | 3.04 | 2.65 |
| GRB7 | 7.2 | 7.27 | 6.64 | 6.58 | 4.09 | 4.16 | 4.20 | 3.75 |
| NID2 | 8.7 | 8.58 | 7.88 | 7.9 | 6.12 | 5.94 | 5.78 | 5.87 |
| ARHGAP29 | 9.13 | 9.05 | 8.26 | 8.34 | 7.82 | 7.58 | 7.41 | 7.52 |
| DNAH1 | 7.6 | 7.33 | 6.78 | 6.85 | 1.66 | 1.95 | 1.63 | 1.96 |
| BCORP1 | 5.4 | 5.27 | 4.91 | 4.83 | 1.38 | 1.70 | 1.43 | 1.19 |
| HECW1 | 7.93 | 7.85 | 7.18 | 7.22 | 4.77 | 3.48 | 4.05 | 3.77 |
| RASSF4 | 9.95 | 9.93 | 9.18 | 8.96 | 5.34 | 5.10 | 3.59 | 4.81 |
| IFI35 | 8.19 | 8.14 | 7.56 | 7.34 | 5.70 | 5.96 | 5.31 | 5.20 |
| NXNL2 | 7.47 | 7.25 | 6.81 | 6.62 | 3.60 | 2.66 | 3.01 | 2.77 |
| BCL3 | 9.79 | 9.71 | 8.89 | 8.9 | 6.14 | 6.36 | 6.03 | 6.09 |
| MAF | 9.8 | 9.81 | 8.99 | 8.9 | 7.43 | 7.51 | 7.49 | 7.33 |
| FAM149A | 7.55 | 7.79 | 6.91 | 7.08 | 2.80 | 3.39 | 2.93 | 2.03 |
| ARSD | 8.83 | 8.75 | 7.9 | 8.13 | 6.15 | 6.09 | 5.67 | 5.84 |
| TBC1D8 | 7.98 | 7.84 | 7.24 | 7.17 | 4.93 | 4.22 | 4.34 | 4.35 |
| OLFML2A | 7.48 | 7.63 | 6.98 | 6.78 | 5.04 | 4.17 | 3.64 | 3.93 |
| TAPT1-AS1 | 5.675 | 5.795 | 5.045 | 5.4 | 2.31 | 2.51 | 2.56 | 2.26 |
| TLL1 | 6.81 | 7.05 | 6.27 | 6.35 | 4.88 | 2.87 | 3.17 | 2.43 |
| TMEM91 | 8.25 | 8.04 | 7.42 | 7.41 | 3.29 | 3.44 | 3.20 | 2.90 |
| MAML2 | 9.01 | 8.87 | 8.12 | 8.15 | 5.57 | 5.35 | 5.45 | 5.09 |
| PER1 | 8.6 | 8.49 | 7.84 | 7.69 | 4.24 | 4.33 | 3.41 | 3.63 |
| MSC | 7.49 | 7.25 | 6.77 | 6.62 | 5.07 | 4.59 | 4.44 | 4.73 |
| PLD1 | 8.05 | 8.09 | 7.31 | 7.34 | 5.67 | 5.36 | 5.14 | 5.47 |
| DMRTA1 | 8.24 | 7.93 | 7.23 | 7.44 | 6.23 | 5.83 | 6.14 | 5.90 |
| HOOK1 | 7.45 | 7.44 | 6.76 | 6.74 | 5.02 | 5.41 | 4.77 | 4.96 |
| DNMT3B | 8.93 | 8.8 | 8.15 | 7.91 | 5.72 | 5.63 | 4.90 | 5.25 |
| TM4SF18 | 10.08 | 10 | 9.13 | 9.05 | 7.66 | 7.56 | 7.20 | 7.74 |
| SORCS2 | 7.6 | 7.4 | 6.78 | 6.8 | 3.57 | 3.61 | 3.19 | 3.72 |
| C1RL | 7.81 | 7.9 | 7.03 | 7.19 | 4.41 | 4.41 | 3.68 | 3.87 |
| FMO4 | 7.22 | 7.01 | 6.45 | 6.43 | 4.67 | 3.65 | 3.83 | 4.10 |

| | | | | | | | | |
|---|---|---|---|---|---|---|---|---|
| GDPD3 | 7.75 | 7.74 | 7.12 | 6.9 | 1.43 | 1.42 | 1.17 | 1.24 |
| RTKN2 | 9.1 | 8.81 | 8.09 | 8.12 | 4.81 | 4.96 | 3.36 | 3.78 |
| H6PD | 8.14 | 8.17 | 7.4 | 7.34 | 4.73 | 4.57 | 3.97 | 3.53 |
| MIR604 | 10.05 | 9.8 | 9.04 | 8.89 | 3.70 | 4.64 | 3.49 | 3.49 |
| PLXND1 | 8.83 | 8.61 | 7.86 | 7.89 | 4.76 | 4.28 | 3.95 | 3.67 |
| HCFC1R1 | 9.3 | 9.19 | 8.48 | 8.21 | 6.14 | 5.89 | 5.73 | 5.91 |
| SVIL | 9.225 | 9.05 | 8.29 | 8.205 | 4.82 | 5.07 | 4.84 | 4.83 |
| EGR2 | 7.31 | 7.35 | 6.6 | 6.63 | 1.96 | 2.07 | 1.96 | 2.03 |
| MIR4803 | 8.83 | 8.89 | 8.04 | 7.95 | 1.16 | 0.35 | 0.43 | 0.72 |
| DDX58 | 9.41 | 9.32 | 8.43 | 8.47 | 5.90 | 5.45 | 5.22 | 5.41 |
| HECW2 | 7.9 | 7.83 | 7.21 | 6.98 | 4.85 | 3.94 | 4.26 | 4.50 |
| LOC553103 | 8.02 | 8.11 | 7.31 | 7.23 | 2.79 | 2.60 | 2.34 | 2.65 |
| TLR3 | 7.21 | 6.96 | 6.43 | 6.34 | 5.06 | 5.15 | 4.86 | 4.09 |
| PPP4R4 | 7.09 | 6.84 | 6.31 | 6.24 | 2.64 | 2.80 | 2.41 | 2.76 |
| PER3 | 9.59 | 9.53 | 8.61 | 8.6 | 5.08 | 5.45 | 3.64 | 4.48 |
| PTPRD | 9.1 | 9.01 | 8.14 | 8.16 | 7.15 | 6.75 | 6.04 | 6.70 |
| MIR181B2 | 7.97 | 7.97 | 7.23 | 7.11 | 4.44 | 4.05 | 4.11 | 4.27 |
| SLC6A13 | 6.99 | 6.88 | 6.21 | 6.26 | 2.29 | 2.37 | 2.04 | 2.21 |
| SGK2 | 9.03 | 8.99 | 8.08 | 8.1 | 5.51 | 5.78 | 5.66 | 5.22 |
| UNC13C | 4.79 | 4.89 | 4.29 | 4.4 | 1.57 | 0.95 | 0.92 | 0.88 |
| PDGFB | 9.11 | 8.86 | 8.07 | 8.05 | 6.24 | 6.20 | 5.19 | 5.05 |
| SLC4A4 | 10.65 | 10.58 | 9.48 | 9.56 | 8.30 | 7.82 | 7.45 | 7.77 |
| ZNF117 | 8.75 | 8.82 | 7.73 | 8.02 | 4.86 | 3.94 | 3.74 | 4.10 |
| LIPG | 9.27 | 9.25 | 8.34 | 8.26 | 5.66 | 6.00 | 3.51 | 3.61 |
| PTGES | 8.15 | 8.15 | 7.36 | 7.25 | 5.01 | 5.04 | 4.08 | 4.32 |
| PCDHGB8P | 6.06 | 6.09 | 5.39 | 5.5 | 2.90 | 2.66 | 2.04 | 2.07 |
| RHPN1 | 7.56 | 7.34 | 6.77 | 6.58 | 2.70 | 3.17 | 2.66 | 2.82 |
| MAP3K8 | 9.24 | 9.255 | 8.365 | 8.185 | 4.39 | 4.57 | 4.31 | 4.23 |
| DLGAP1-AS3 | 5.87 | 6.08 | 5.38 | 5.31 | 0.88 | 1.36 | 1.15 | 1.05 |
| CCDC146 | 7.08 | 6.98 | 6.23 | 6.32 | 3.04 | 3.16 | 2.94 | 2.61 |
| SFRP4 | 5.79 | 5.93 | 5.1 | 5.36 | 3.51 | 3.00 | 2.61 | 3.63 |
| ATP1B1 | 11.39 | 11.32 | 10.14 | 10.11 | 9.56 | 9.36 | 9.03 | 9.11 |
| MITF | 7.96 | 7.98 | 7.07 | 7.14 | 5.40 | 5.36 | 5.32 | 5.38 |
| ARSD-AS1 | 6.34 | 6.05 | 5.55 | 5.49 | 2.24 | 2.39 | 1.97 | 1.84 |
| ABCC6 | 7.6 | 7.62 | 6.79 | 6.77 | 2.65 | 3.94 | 2.62 | 3.34 |
| MAMDC4 | 9.32 | 9.16 | 8.25 | 8.2 | 2.45 | 2.78 | 2.40 | 2.57 |
| IFIH1 | 8.2 | 7.91 | 7.26 | 7.08 | 4.82 | 4.57 | 4.60 | 4.40 |
| PLEKHH2 | 7.44 | 7.57 | 6.71 | 6.65 | 3.76 | 2.64 | 3.15 | 2.82 |
| MCTP1 | 7.55 | 7.53 | 6.8 | 6.62 | 5.18 | 4.24 | 2.76 | 2.73 |
| P2RX4 | 7.55 | 7.68 | 6.82 | 6.73 | 3.87 | 3.73 | 3.44 | 3.87 |
| UBA7 | 9.28 | 9.18 | 8.25 | 8.16 | 5.13 | 5.13 | 4.72 | 5.09 |
| MTMR11 | 9.07 | 8.92 | 7.94 | 8.04 | 3.47 | 3.14 | 3.37 | 3.14 |
| KBTBD3 | 7.04 | 6.83 | 6.22 | 6.1 | 2.90 | 2.11 | 2.28 | 2.13 |
| NEFL | 11.96 | 11.87 | 10.58 | 10.58 | 9.92 | 9.71 | 9.84 | 9.75 |
| S1PR1 | 7.43 | 7.02 | 6.53 | 6.3 | 8.34 | 7.15 | 7.53 | 7.60 |
| TNFAIP3 | 9.11 | 8.99 | 8.03 | 8.04 | 6.21 | 5.78 | 4.31 | 4.66 |
| FOXP2 | 8.43 | 8.13 | 7.27 | 7.43 | 4.72 | 4.59 | 4.65 | 4.26 |
| ARSE | 7.73 | 7.64 | 6.78 | 6.86 | 3.14 | 3.43 | 3.01 | 3.15 |
| ANKS1B | 6.68 | 6.49 | 5.83 | 5.84 | 2.74 | 2.99 | 2.81 | 2.41 |
| ESX1 | 5.27 | 5.48 | 4.79 | 4.73 | 1.31 | 1.42 | 1.19 | 1.25 |
| BCL2L11 | 8.99 | 8.73 | 7.86 | 7.82 | 4.67 | 4.25 | 4.30 | 4.58 |
| EPB41L4A | 7.67 | 7.53 | 6.71 | 6.73 | 5.70 | 5.86 | 5.47 | 5.59 |
| GLCCI1 | 7.59 | 7.52 | 6.71 | 6.65 | 4.12 | 4.35 | 3.95 | 4.05 |
| SMR3A | 6.37 | 6.4 | 5.67 | 5.62 | 1.06 | 0.96 | 0.79 | 1.21 |
| WDR78 | 7.32 | 7.18 | 6.55 | 6.26 | 3.07 | 2.82 | 2.92 | 2.74 |
| B3GNT4 | 9.53 | 9.34 | 8.35 | 8.29 | 4.71 | 5.03 | 4.51 | 4.53 |

| | | | | | | | | |
|---|---|---|---|---|---|---|---|---|
| GUCA1C | 4.3 | 4.48 | 3.92 | 3.82 | 2.57 | 2.00 | 1.33 | 1.74 |
| TRIM22 | 8.74 | 8.86 | 7.9 | 7.61 | 5.11 | 4.44 | 4.15 | 4.03 |
| CNR1 | 5.82 | 5.62 | 5.105 | 4.975 | 4.33 | 2.90 | 3.28 | 3.59 |
| JAM2 | 5.52 | 5.81 | 5.06 | 4.89 | 1.39 | 1.34 | 0.99 | 0.98 |
| ADAMTS9-AS2 | 6.74 | 6.79 | 5.81 | 6.05 | 3.05 | 1.66 | 2.90 | 1.62 |
| F8 | 6.21 | 6.38 | 5.46 | 5.56 | 2.54 | 2.17 | 2.38 | 2.15 |
| FHDC1 | 7.23 | 7.04 | 6.34 | 6.15 | 4.46 | 4.06 | 3.46 | 3.56 |
| HSD17B7P2 | 8.51 | 8.35 | 7.45 | 7.3 | 5.05 | 4.78 | 3.91 | 4.06 |
| ACTR3C | 9.9 | 9.76 | 8.55 | 8.62 | 6.69 | 6.32 | 6.04 | 6.12 |
| SLN | 8.43 | 8.44 | 7.25 | 7.47 | 5.40 | 5.88 | 5.05 | 5.11 |
| HNF1A-AS1 | 7.2 | 7.08 | 6.06 | 6.4 | 1.95 | 2.34 | 1.67 | 1.24 |
| DAPK1 | 10.97 | 10.89 | 9.56 | 9.51 | 8.36 | 8.42 | 7.76 | 8.00 |
| SLC16A4 | 9 | 8.64 | 7.68 | 7.7 | 7.04 | 6.41 | 6.50 | 6.65 |
| PRRT2 | 6.94 | 7.02 | 6.01 | 6.16 | 1.72 | 2.28 | 1.43 | 1.06 |
| OAS2 | 7.53 | 7.43 | 6.67 | 6.35 | 2.48 | 2.86 | 2.62 | 2.37 |
| MMP1 | 6.2 | 6.37 | 5.44 | 5.49 | 1.25 | 1.20 | 1.29 | 0.91 |
| FBXL13 | 7.02 | 6.6 | 5.89 | 5.94 | 4.16 | 3.45 | 3.30 | 3.73 |
| SLC44A3 | 8.02 | 7.95 | 6.91 | 6.96 | 5.33 | 4.65 | 4.80 | 5.18 |
| EGR1 | 9.61 | 9.44 | 8.26 | 8.27 | 4.00 | 4.92 | 3.46 | 4.49 |
| VASN | 8.28 | 8.29 | 7.1 | 7.25 | 4.79 | 4.86 | 4.53 | 4.43 |
| SIPA1L2 | 9.82 | 9.78 | 8.4 | 8.57 | 6.15 | 5.89 | 6.14 | 5.66 |
| PLCB1 | 7.11 | 6.96 | 5.96 | 6.22 | 3.74 | 3.45 | 2.80 | 2.43 |
| PRKCQ | 6.01 | 5.93 | 5.16 | 5.17 | 2.49 | 2.03 | 1.57 | 2.38 |
| MAP7D2 | 9.6 | 9.54 | 8.29 | 8.26 | 7.18 | 7.20 | 6.81 | 7.22 |
| GBP2 | 5.86 | 5.725 | 5.055 | 4.96 | 3.14 | 3.05 | 2.44 | 2.65 |
| MTSS1 | 10.48 | 10.42 | 9.02 | 9.04 | 6.07 | 6.39 | 4.82 | 5.25 |
| CP | 10.47 | 10.47 | 9.02 | 9.07 | 6.72 | 6.22 | 2.71 | 4.02 |
| SAMD9L | 9.58 | 9.57 | 8.29 | 8.24 | 6.52 | 5.90 | 6.32 | 6.08 |
| DSCAML1 | 8.2 | 8.15 | 6.95 | 7.15 | 3.26 | 4.06 | 2.96 | 3.57 |
| QPRT | 8.82 | 8.64 | 7.53 | 7.51 | 8.33 | 7.72 | 7.28 | 7.29 |
| KANSL1L | 9.13 | 9.04 | 7.87 | 7.78 | 4.82 | 3.64 | 4.14 | 4.24 |
| RASSF9 | 7.51 | 7.34 | 6.5 | 6.29 | 4.67 | 4.04 | 4.38 | 3.98 |
| FGFR4 | 8.33 | 8.37 | 7.03 | 7.33 | 6.06 | 5.24 | 4.62 | 4.69 |
| OLFML2B | 8.62 | 8.39 | 7.47 | 7.15 | 4.59 | 4.93 | 3.65 | 4.24 |
| EDN1 | 9.15 | 9.1 | 7.98 | 7.7 | 7.49 | 8.14 | 6.12 | 7.06 |
| DCLK1 | 7.83 | 7.49 | 6.51 | 6.62 | 5.44 | 5.75 | 5.53 | 5.13 |
| VSTM4 | 9.34 | 9.13 | 7.79 | 8.02 | 4.48 | 4.43 | 4.26 | 4.13 |
| LOC441204 | 8.8 | 8.73 | 7.53 | 7.45 | 3.62 | 3.08 | 2.87 | 3.30 |
| RNF144B | 7.82 | 7.71 | 6.68 | 6.59 | 5.58 | 5.23 | 4.93 | 4.37 |
| ZHX2 | 10.58 | 10.43 | 8.93 | 9.02 | 7.75 | 7.82 | 7.60 | 7.79 |
| FRMD4B | 7.32 | 7.29 | 6.26 | 6.21 | 4.22 | 4.07 | 3.64 | 3.74 |
| PTPN13 | 10.99 | 10.89 | 9.33 | 9.34 | 9.10 | 8.56 | 8.75 | 8.90 |
| IL1R1 | 9.98 | 9.71 | 8.48 | 8.29 | 6.38 | 5.96 | 5.71 | 5.90 |
| MIR3974 | 5.08 | 4.93 | 4.23 | 4.29 | 0.82 | 0.99 | 0.76 | 0.68 |
| DHRS9 | 5.96 | 5.83 | 5.03 | 4.99 | 1.46 | 1.37 | 1.26 | 1.04 |
| BCL2 | 7.9 | 7.55 | 6.67 | 6.46 | 6.39 | 5.22 | 5.40 | 5.39 |
| CD24 | 12.49 | 12.51 | 10.55 | 10.69 | 9.82 | 9.90 | 9.61 | 9.94 |
| NPY1R | 6.71 | 6.54 | 5.61 | 5.64 | 4.55 | 3.51 | 3.55 | 3.90 |
| STAT1 | 12.65 | 12.59 | 10.69 | 10.69 | 9.89 | 9.62 | 9.23 | 9.39 |
| ITPR1 | 9.45 | 9.33 | 7.97 | 7.92 | 5.57 | 5.63 | 4.91 | 5.09 |
| SEMA3A | 7.79 | 7.46 | 6.37 | 6.53 | 6.69 | 5.49 | 5.83 | 5.69 |
| PELI1 | 8.67 | 8.52 | 7.25 | 7.29 | 6.83 | 6.39 | 6.00 | 5.67 |
| HNF1B | 12 | 11.89 | 10.05 | 10.11 | 9.29 | 9.04 | 9.01 | 9.24 |
| SEMA6D | 7.94 | 7.78 | 6.64 | 6.61 | 5.14 | 4.70 | 5.05 | 4.57 |
| SPINK13 | 5.59 | 5.25 | 4.75 | 4.37 | 2.43 | 1.23 | 1.20 | 1.57 |
| FRK | 7.66 | 7.63 | 6.36 | 6.47 | 6.11 | 5.72 | 5.48 | 5.07 |

| | | | | | | | | |
|---|---|---|---|---|---|---|---|---|
| CST1 | 4.46 | 4.28 | 3.56 | 3.77 | 2.90 | 0.77 | 0.49 | 0.70 |
| DGCR9 | 7.56 | 7.19 | 6.4 | 5.97 | 1.61 | 2.61 | 1.69 | 2.01 |
| FCAMR | 7.31 | 7.43 | 6.12 | 6.24 | 2.53 | 2.72 | 1.96 | 1.65 |
| MS4A3 | 4.68 | 4.7 | 3.83 | 4.03 | 0.94 | 1.01 | 0.89 | 1.04 |
| ARL14EPL | 7.16 | 7.22 | 6.01 | 6.01 | 5.56 | 5.59 | 5.09 | 4.47 |
| CA2 | 10.4 | 10.23 | 8.59 | 8.64 | 6.90 | 6.14 | 5.97 | 6.40 |
| SEMA6A | 9.86 | 9.86 | 8.18 | 8.28 | 5.77 | 5.84 | 5.00 | 5.04 |
| CDKL5 | 10.66 | 10.59 | 8.85 | 8.88 | 7.36 | 7.13 | 6.74 | 7.00 |
| DNAJB13 | 5.67 | 5.55 | 4.9 | 4.46 | 2.13 | 1.07 | 0.83 | 1.43 |
| ASTN2 | 7.58 | 7.66 | 6.37 | 6.34 | 3.70 | 3.79 | 3.32 | 3.52 |
| SORBS1 | 9.49 | 9.38 | 7.85 | 7.87 | 4.98 | 5.00 | 4.41 | 4.12 |
| C10orf62 | 7.9 | 7.69 | 6.41 | 6.54 | 3.23 | 2.96 | 2.73 | 3.24 |
| SEMA5B | 9.14 | 9 | 7.59 | 7.46 | 4.28 | 4.27 | 3.37 | 4.56 |
| ZSCAN31 | 7.46 | 7.58 | 6.25 | 6.21 | 4.20 | 3.73 | 4.08 | 3.80 |
| MBL2 | 6.61 | 6.59 | 5.54 | 5.38 | 2.95 | 2.60 | 1.34 | 1.62 |
| OR1F1 | 5 | 5.18 | 4.12 | 4.3 | 1.28 | 1.06 | 0.51 | 0.90 |
| AGMO | 6.73 | 6.53 | 5.6 | 5.35 | 2.21 | 1.59 | 1.44 | 1.20 |
| BIRC3 | 10.27 | 10.15 | 8.42 | 8.44 | 6.24 | 6.75 | 5.33 | 5.35 |
| TRABD2B | 8.41 | 8.14 | 6.86 | 6.8 | 3.69 | 3.59 | 3.74 | 3.16 |
| NCKAP5 | 8.17 | 8.17 | 6.69 | 6.77 | 3.33 | 4.33 | 3.83 | 3.67 |
| MIR3936 | 6.37 | 6.27 | 5.08 | 5.27 | 2.21 | 2.74 | 2.16 | 1.95 |
| C1orf186 | 8.26 | 8.07 | 6.68 | 6.69 | 4.65 | 4.38 | 3.23 | 4.05 |
| LOC100506895 | 6.66 | 6.65 | 5.69 | 5.2 | 5.26 | 5.95 | 4.16 | 5.21 |
| CYP1B1 | 9.27 | 9.21 | 7.51 | 7.59 | 6.60 | 8.38 | 5.77 | 6.00 |
| SGPP2 | 8.36 | 8.36 | 6.74 | 6.91 | 5.72 | 5.51 | 3.60 | 3.73 |
| GMNC | 7.33 | 7.37 | 5.69 | 6.31 | 2.35 | 3.27 | 1.78 | 1.77 |
| LINC00410 | 5.48 | 5.28 | 4.52 | 4.26 | 0.80 | 0.83 | 0.80 | 0.72 |
| OAS1 | 7.73 | 7.74 | 6.4 | 6.22 | 3.45 | 3.25 | 3.11 | 2.97 |
| LOC440300 | 5.26 | 4.99 | 4.22 | 4.14 | 0.58 | 0.92 | 0.61 | 0.76 |
| GABRG1 | 4.26 | 4.3 | 3.37 | 3.6 | 1.17 | 0.97 | 1.05 | 0.78 |
| CTSO | 6.55 | 6.78 | 5.38 | 5.46 | 4.87 | 4.26 | 4.54 | 3.83 |
| EFHB | 6.65 | 6.35 | 5.27 | 5.27 | 4.28 | 1.98 | 1.95 | 1.96 |
| SAA1 | 5.88 | 6.05 | 4.9 | 4.77 | 5.85 | 5.64 | 5.22 | 5.41 |
| PLEK | 7.73 | 7.66 | 6.4 | 6.06 | 4.91 | 4.83 | 4.53 | 4.74 |
| C14orf105 | 9.32 | 9.25 | 7.45 | 7.54 | 5.94 | 5.03 | 5.62 | 5.08 |
| LHFPL3-AS2 | 6.39 | 6.83 | 5.45 | 5.22 | 1.99 | 1.06 | 0.89 | 1.62 |
| SMPDL3A | 10.09 | 9.93 | 7.98 | 8.13 | 5.92 | 5.62 | 4.15 | 4.61 |
| GPRIN3 | 8.4 | 8.11 | 6.67 | 6.5 | 4.01 | 3.05 | 3.12 | 3.03 |
| IMPA2 | 8.19 | 7.97 | 6.28 | 6.6 | 7.76 | 6.94 | 6.48 | 6.91 |
| GPRC5B | 9.36 | 9.18 | 7.48 | 7.19 | 7.21 | 6.66 | 6.19 | 6.32 |
| SLC2A2 | 5.64 | 5.7 | 4.27 | 4.69 | 1.92 | 1.59 | 1.11 | 0.76 |
| MIR1302-7 | 3.23 | 3.08 | 2.57 | 2.39 | 1.75 | 0.79 | 0.89 | 1.34 |
| LRRC37A3 | 9.24 | 9.02 | 7.14 | 7.2 | 5.96 | 5.48 | 3.65 | 3.39 |
| TNFAIP6 | 7.84 | 7.81 | 6.2 | 6 | 5.55 | 4.41 | 2.49 | 3.51 |
| ACMSD | 6.93 | 6.97 | 5.32 | 5.5 | 3.32 | 1.61 | 2.10 | 1.18 |
| VCAM1 | 9.61 | 9.51 | 7.53 | 7.31 | 8.24 | 8.11 | 5.24 | 5.29 |
| CCL2 | 10.79 | 10.66 | 8.47 | 8.1 | 8.38 | 7.65 | 2.83 | 4.19 |
| ATP8A1 | 7.82 | 7.85 | 6.12 | 5.96 | 5.70 | 4.88 | 5.09 | 4.90 |
| VAV3 | 6.66 | 6.16 | 4.85 | 4.85 | 1.85 | 1.78 | 1.12 | 1.31 |
| MAB21L3 | 7.5 | 7.51 | 5.96 | 5.39 | 4.77 | 4.73 | 3.65 | 2.84 |
| CLEC4E | 6.65 | 6.84 | 4.91 | 5.29 | 4.68 | 3.53 | 2.27 | 1.60 |
| MIR516B2 | 3.62 | 4.02 | 2.99 | 2.71 | 0.95 | 1.54 | 1.16 | 1.08 |
| CXCL8 | 8.82 | 8.85 | 6.46 | 6.71 | 5.19 | 5.34 | 4.32 | 4.18 |
| C3 | 8.92 | 8.87 | 6.55 | 6.58 | 5.10 | 4.06 | 3.08 | 2.81 |
| KIF12 | 9.86 | 9.27 | 7.19 | 6.86 | 4.71 | 4.69 | 4.50 | 4.61 |
| SLC17A1 | 6.38 | 6.23 | 4.62 | 4.32 | 2.80 | 2.69 | 2.51 | 1.59 |

| | | | | | | | | |
|---|---|---|---|---|---|---|---|---|
| TINAG | 8 | 8.09 | 5.66 | 5.65 | 2.69 | 2.17 | 1.38 | 1.76 |
| ITGB6 | 8.67 | 8.46 | 5.92 | 6.08 | 6.90 | 4.57 | 5.63 | 5.81 |
| IFI44L | 8.7 | 8.65 | 6.19 | 5.88 | 4.19 | 2.84 | 2.71 | 2.21 |
| ENPP3 | 8.94 | 8.64 | 5.87 | 5.78 | 3.62 | 3.03 | 2.51 | 2.80 |
| ABCA12 | 8.95 | 8.86 | 5.94 | 5.79 | 6.78 | 5.95 | 5.64 | 5.56 |

**Table S5. Microarray (LogFC value) and prognosis data (Cox q-value) for 32 genes coordinately activated by both ZHX2 and RelA/p65, in which higher expression was associated with worse prognosis of ccRCC**

| Gene | ZHX2_scr1 | ZHX2_scr2 | ZHX2_sh45_1 | ZHX2_sh45_2 | p65_scr1 | p65_scr2 | p65_sh1 | p65_sh2 | **Cox q-value** |
|---|---|---|---|---|---|---|---|---|---|
| PHF21A | 9.32 | 9.13 | 8.72 | 8.67 | 6.79 | 6.74 | 6.08 | 6.32 | 3.4659E-06 |
| MOV10 | 10.77 | 10.62 | 10.02 | 10.06 | 7.61 | 7.40 | 7.09 | 7.16 | 9.47605E-07 |
| C1RL | 7.81 | 7.9 | 7.03 | 7.19 | 4.41 | 4.41 | 3.68 | 3.87 | 8.05148E-08 |
| RBCK1 | 10.72 | 10.84 | 10.35 | 10.29 | 7.68 | 7.81 | 7.78 | 7.50 | 2.21016E-07 |
| NLGN2 | 9.005 | 8.9 | 8.55 | 8.49 | 5.24 | 4.98 | 5.07 | 4.98 | 3.48406E-06 |
| TMEM234 | 8.56 | 8.55 | 8.04 | 8.01 | 3.82 | 4.25 | 4.09 | 3.68 | 9.75958E-05 |
| IKBKE | 8.4 | 8.34 | 7.74 | 7.71 | 5.42 | 5.35 | 4.34 | 4.46 | 2.21016E-07 |
| BCL3 | 9.79 | 9.71 | 8.89 | 8.9 | 6.14 | 6.36 | 6.03 | 6.09 | 5.13597E-07 |
| DLGAP1-AS1 | 8.27 | 7.98 | 7.47 | 7.49 | 4.79 | 5.36 | 4.98 | 4.95 | 0.000284693 |
| HOXA3 | 8.47 | 8.47 | 7.91 | 7.73 | 6.45 | 6.43 | 6.44 | 6.42 | 2.87515E-06 |
| TMEM132A | 8.55 | 8.57 | 7.96 | 7.97 | 4.79 | 4.31 | 4.58 | 3.65 | 6.01353E-07 |
| PORCN | 10.58 | 10.47 | 9.85 | 9.88 | 7.55 | 8.40 | 7.63 | 7.67 | 0.000979143 |
| DNMT3B | 8.93 | 8.8 | 8.15 | 7.91 | 5.72 | 5.63 | 4.90 | 5.25 | 1.60869E-05 |
| MAP3K8 | 9.24 | 9.255 | 8.365 | 8.185 | 4.39 | 4.57 | 4.31 | 4.23 | 8.28719E-05 |
| RHPN1 | 7.56 | 7.34 | 6.77 | 6.58 | 2.70 | 3.17 | 2.66 | 2.82 | 2.20608E-05 |
| ZNF83 | 10.01 | 9.82 | 9.16 | 9.27 | 4.24 | 4.01 | 3.90 | 4.08 | 0.00021173 |
| RTKN2 | 9.1 | 8.81 | 8.09 | 8.12 | 4.81 | 4.96 | 3.36 | 3.78 | 0.000226824 |
| TAPT1-AS1 | 5.675 | 5.795 | 5.045 | 5.4 | 2.31 | 2.51 | 2.56 | 2.26 | 0.00269226 |
| VASN | 8.28 | 8.29 | 7.1 | 7.25 | 4.79 | 4.86 | 4.53 | 4.43 | 0.003585338 |
| TGFB1 | 10.9 | 10.77 | 10.34 | 10.26 | 9.05 | 8.63 | 8.54 | 8.40 | 0.009264931 |
| MSC | 7.49 | 7.25 | 6.77 | 6.62 | 5.07 | 4.59 | 4.44 | 4.73 | 2.41333E-05 |
| XAF1 | 9.4 | 9.45 | 8.8 | 8.92 | 5.48 | 5.54 | 5.39 | 5.01 | 0.00026708 |
| PLEKHG2 | 8.55 | 8.47 | 8.08 | 7.98 | 4.84 | 4.45 | 4.74 | 4.39 | 0.008740881 |
| ACTR3C | 9.9 | 9.76 | 8.55 | 8.62 | 6.69 | 6.32 | 6.04 | 6.12 | 0.007432824 |
| GCNT1 | 10.32 | 10.16 | 9.41 | 9.45 | 7.31 | 7.20 | 6.74 | 6.82 | 0.006958367 |
| SEMA3A | 7.79 | 7.46 | 6.37 | 6.53 | 6.69 | 5.49 | 5.83 | 5.69 | 0.000526718 |
| CTHRC1 | 7.66 | 7.58 | 6.95 | 7.16 | 5.55 | 5.28 | 4.35 | 4.67 | 0.000376094 |
| CYP1B1 | 9.27 | 9.21 | 7.51 | 7.59 | 6.60 | 8.38 | 5.77 | 6.00 | 0.000958604 |
| MUC1 | 7.43 | 7.34 | 6.82 | 6.75 | 3.55 | 4.70 | 3.28 | 3.61 | 0.003382318 |
| PRRT2 | 6.94 | 7.02 | 6.01 | 6.16 | 1.72 | 2.28 | 1.43 | 1.06 | 0.006537995 |
| GXYLT2 | 10.67 | 10.66 | 9.84 | 9.82 | 8.09 | 8.08 | 7.03 | 7.17 | 0.004657458 |
| IL6 | 7.68 | 7.92 | 7.08 | 7.23 | 4.31 | 5.03 | 3.12 | 3.12 | 4.87762E-05 |

**References**


31. L. Li *et al.*, Hypoxia-inducible factor linked to differential kidney cancer risk seen with type 2A and type 2B VHL mutations. *Mol Cell Biol* **27**, 5381-5392 (2007).
32. H. Yang, M. Ivan, J. H. Min, W. Y. Kim, W. G. Kaelin, Jr., Analysis of von Hippel-Lindau hereditary cancer syndrome: implications of oxygen sensing. *Methods in enzymology* **381**, 320-335 (2004).
33. D. Wang, A. S. Baldwin, Jr., Activation of nuclear factor-kappaB-dependent transcription by tumor necrosis factor-alpha is mediated through phosphorylation of RelA/p65 on serine 529. *The Journal of biological chemistry* **273**, 29411-29416 (1998).
34. M. F. Kendellen, J. W. Bradford, C. L. Lawrence, K. S. Clark, A. S. Baldwin, Canonical and non-canonical NF-kappaB signaling promotes breast cancer tumor-initiating cells. *Oncogene* **33**, 1297-1305 (2014).
35. Q. Zhang *et al.*, Control of cyclin D1 and breast tumorigenesis by the EglN2 prolyl hydroxylase. *Cancer Cell* **16**, 413-424 (2009).
36. J. Zhang, M. M. Hu, Y. Y. Wang, H. B. Shu, TRIM32 protein modulates type I interferon induction and cellular antiviral response by targeting MITA/STING protein for K63-linked ubiquitination. *J Biol Chem* **287**, 28646-28655 (2012).
37. X. Chen *et al.*, XBP1 promotes triple-negative breast cancer by controlling the HIF1alpha pathway. *Nature* **508**, 103-107 (2014).
38. R. Lu *et al.*, Epigenetic Perturbations by Arg882-Mutated DNMT3A Potentiate Aberrant Stem Cell Gene-Expression Program and Acute Leukemia Development. *Cancer cell* **30**, 92-107 (2016).
39. Y. Zhang *et al.*, Model-based analysis of ChIP-Seq (MACS). *Genome biology* **9**, R137 (2008).
40. T. Lassmann, Y. Hayashizaki, C. O. Daub, TagDust-a program to eliminate artifacts from next generation sequencing data. *Bioinformatics* **25**, 2839-2840 (2009).
41. T. D. Wu, S. Nacu, Fast and SNP-tolerant detection of complex variants and splicing in short reads. *Bioinformatics* **26**, 873-881 (2010).
42. Encode Project Consortium, An integrated encyclopedia of DNA elements in the human genome. *Nature* **489**, 57-74 (2012).
43. S. Heinz *et al.*, Simple combinations of lineage-determining transcription factors prime cis-regulatory elements required for macrophage and B cell identities. *Molecular cell* **38**, 576-589 (2010).
44. T. M. Therneau, P. M. Grambsch, *Modeling survival data : extending the Cox model*. Statistics for biology and health (Springer, New York, 2000), pp. xiii, 350 p.
45. F. E. Harrell, Jr., K. L. Lee, R. M. Califf, D. B. Pryor, R. A. Rosati, Regression modelling strategies for improved prognostic prediction. *Stat Med* **3**, 143-152 (1984).
46. L. Li *et al.*, SQSTM1 is a pathogenic target of 5q copy number gains in kidney cancer. *Cancer Cell* **24**, 738-750 (2013).

47. J. Zhang *et al.*, EglN2 associates with the NRF1-PGC1alpha complex and controls mitochondrial function in breast cancer. *EMBO J* **34**, 2953-2970 (2015).
48. X. Zhao *et al.*, Combined Targeted DNA Sequencing in Non-Small Cell Lung Cancer (NSCLC) Using UNCseq and NGScopy, and RNA Sequencing Using UNCqeR for the Detection of Genetic Aberrations in NSCLC. *PloS one* **10**, e0129280 (2015).
49. X. D. Liu *et al.*, Autophagy mediates HIF2alpha degradation and suppresses renal tumorigenesis. *Oncogene* **34**, 2450-2460 (2015).
50. C. P. Han *et al.*, Scoring of p16(INK4a) immunohistochemistry based on independent nuclear staining alone can sufficiently distinguish between endocervical and endometrial adenocarcinomas in a tissue microarray study. *Mod Pathol* **22**, 797-806 (2009).
51. B. A. Seifert *et al.*, Germline Analysis from Tumor-Germline Sequencing Dyads to Identify Clinically Actionable Secondary Findings. *Clin Cancer Res* **22**, 4087-4094 (2016).
52. W. Huang da, B. T. Sherman, R. A. Lempicki, Systematic and integrative analysis of large gene lists using DAVID bioinformatics resources. *Nat Protoc* **4**, 44-57 (2009).